MAX-PLANCK-INSTITUT FÜR PLASMAPHYSIK

TFIII O2.D4 – Radiation asymmetries

W7-X Workshop

G Partesotti, F Reimold, D Zhang, A Tsikouras, and the W7-X team

This work has been carried out within the framework of the EUROfusion Consortium, funded by the European Union via the Euratom Research and Training Programme (Grant Agreement No 101052200 — EUROfusion). Views and opinions expressed are however those of the author(s) only and do not necessarily reflect those of the European Union or the European Commission. Neither the European Union nor the European Commission can be held responsible for them.

TF-III Main Objectives of OP2.1

- **O1: Core transport and stability**
  - D1: Documentation of profiles for transport analysis and modeling
  - D2: Turbulence in plasma scenario of magnetic configuration (MC) space
  - D3: Impurity transport and perturbative experiments
  - D4: Neoclassic optimization at increased Ti
  - D5: Reduced equilibrium currents at higher beta and in MC space
  - D6: MHD stability and modes in the MC space
- **O2: Edge and SOL transport**
  - D1: Transport across LCFS and in island divertor SOL
  - D2: Validation of edge transport codes
  - D3: SOL width and target heat flux scalings
  - D4: Asymmetries and mapping of diagnostics in 3D SOL
- **O3: Low-field high beta scenarios**
  - D1: Optimization criteria at increased beta
  - D2: High-beta plasma profiles, magnetic fluctuations
  - D3: Field stochastization and implications for SOL / divertor

TF-III Main Objectives of OP2.1

- **O1: Core transport and stability**
  - D1: Documentation of profiles for transport analysis and modeling
  - D2: Turbulence in plasma scenario of magnetic configuration (MC) space
  - D3: Impurity transport and perturbative experiments
  - D4: Neoclassic optimization at increased Ti
  - D5: Reduced equilibrium currents at higher beta and in MC space
  - D6: MHD stability and modes in the MC space
- **O2: Edge and SOL transport**
  - D1: Transport across LCFS and in island divertor SOL
  - D2: Validation of edge transport codes
  - D3: SOL width and target heat flux scalings
  - D4: Asymmetries and mapping of diagnostics in 3D SOL
- **O3: Low-field high beta scenarios**
  - D1: Optimization criteria at increased beta
  - D2: High-beta plasma profiles, magnetic fluctuations
  - D3: Field stochastization and implications for SOL / divertor

Characterization of asymmetries of plasma conditions and radiation, mapping of diagnostic results in 3D island divertor

Poloidal asymmetry

- **Up/down asymmetry of plasma ε**
- **Asymmetry reverses with field reversal**
- Observed also in impurity concentration, target loads, density …

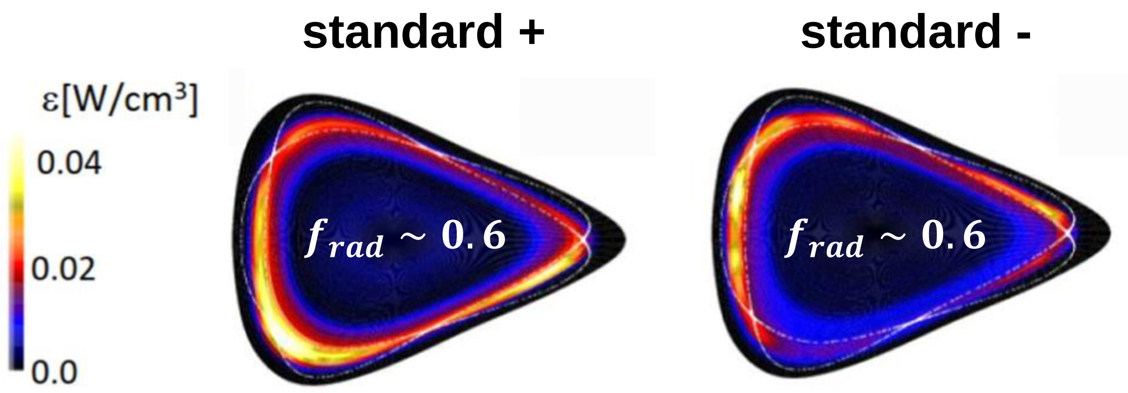

D. Zhang *et al* 2021 *Nucl. Fusion* **61** 126002

Poloidal asymmetry

- **Up/down asymmetry of plasma ε**
- **Asymmetry reverses with field reversal**
- Observed also in impurity concentration, target loads, density …
- **Relevant for: impurity transport, power exhaust**

- **What about other configurations?**
- **Is P_{rad} response from seeding asymmetric?**

standard + **standard -**

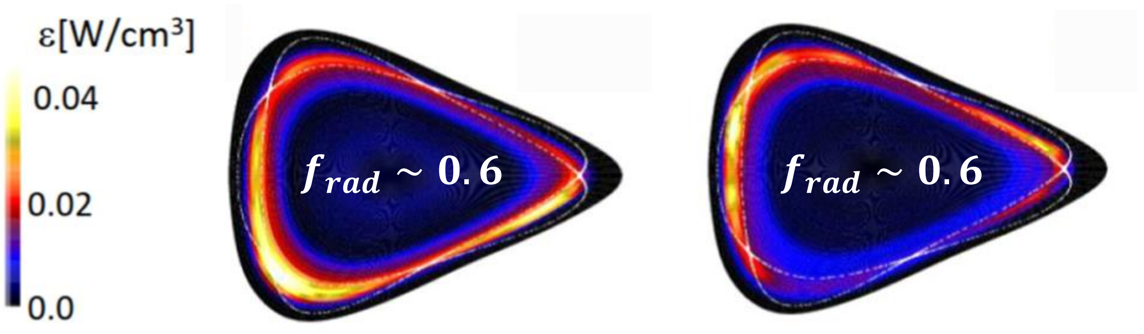

D. Zhang *et al* 2021 *Nucl. Fusion* **61** 126002

standard +

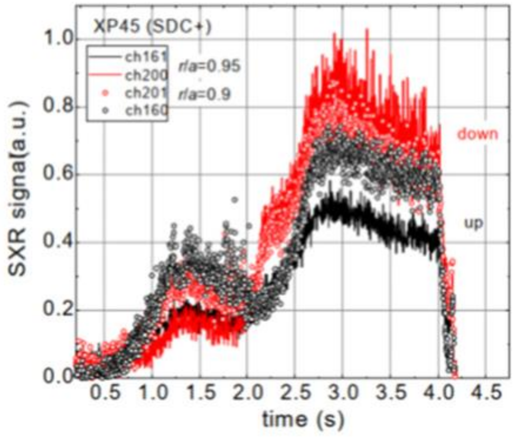

standard -

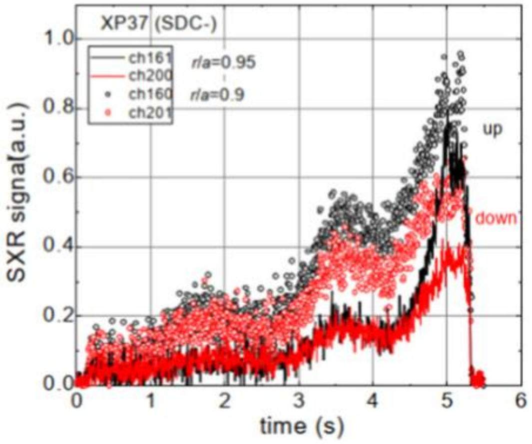

Toroidal asymmetry

- **Expected from EMC3-EIRENE results**
  - Caused by asymmetries in target conditions
  - **P_{rad} peaks at $\varphi = 4°$**
  - In real case, drifts affect the profile

Do we observe this in W7-X?

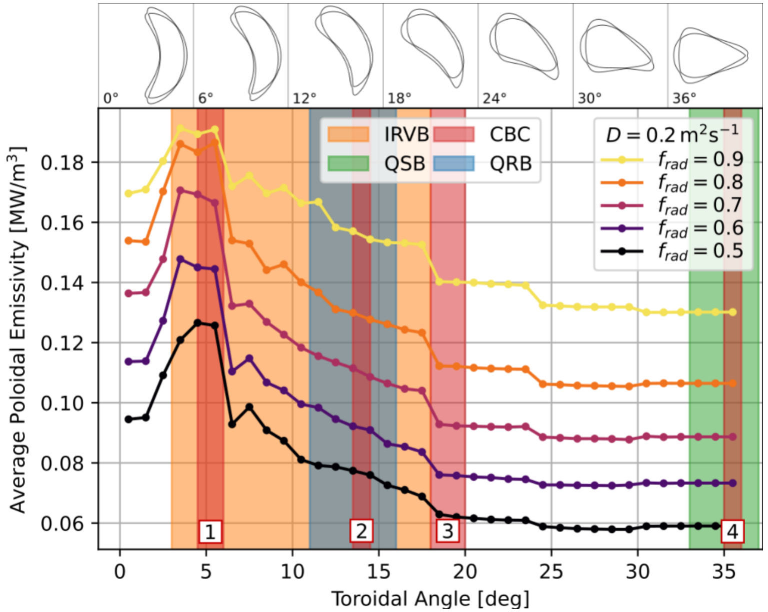

G. Partesotti *in preparation*

Toroidal asymmetry

- **Expected from EMC3-EIRENE results**
  - Caused by asymmetries in target conditions
  - P_{rad} **peaks at** $\varphi = 4°$
  - In real case, drifts affect the profile

- **With impurity seeding**
  - Observed in LHD
  - P_{rad} **peaks 60° in –B direction**
  - Likely caused by drifts

Do we observe this in W7-X?

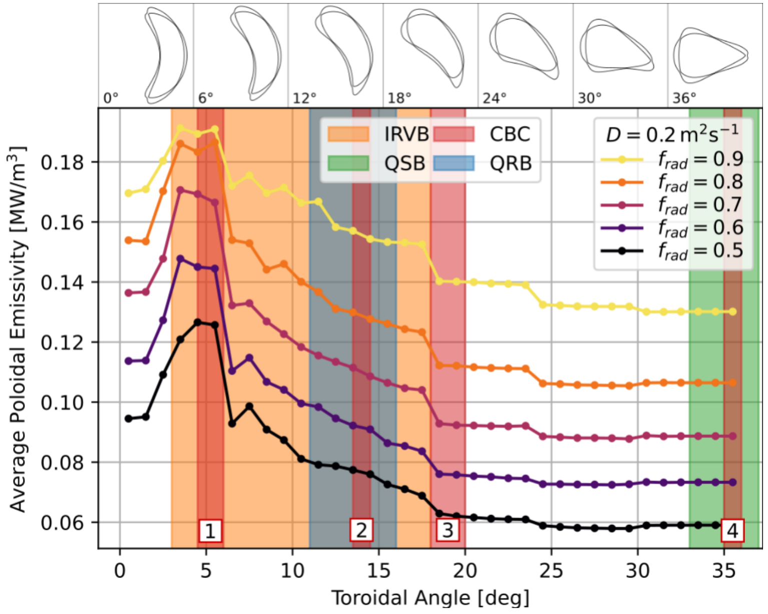

G. Partesotti *in preparation*

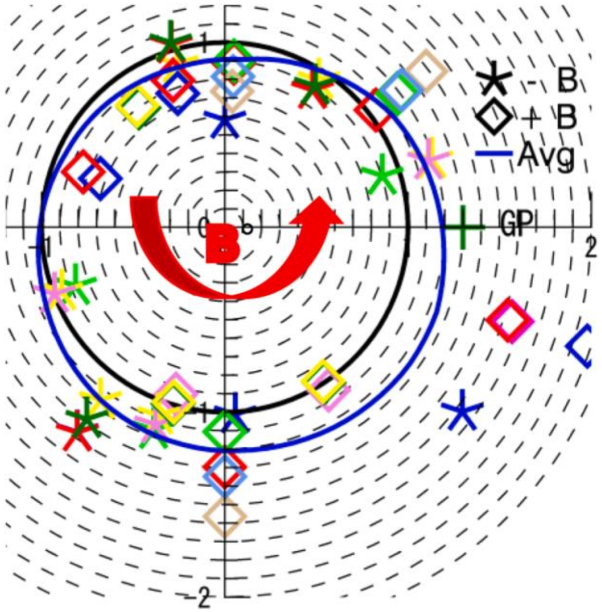

B. J. Peterson et al. 2021 *Nucl. Mat. and Energy* **26** 100848

OP2.1 results

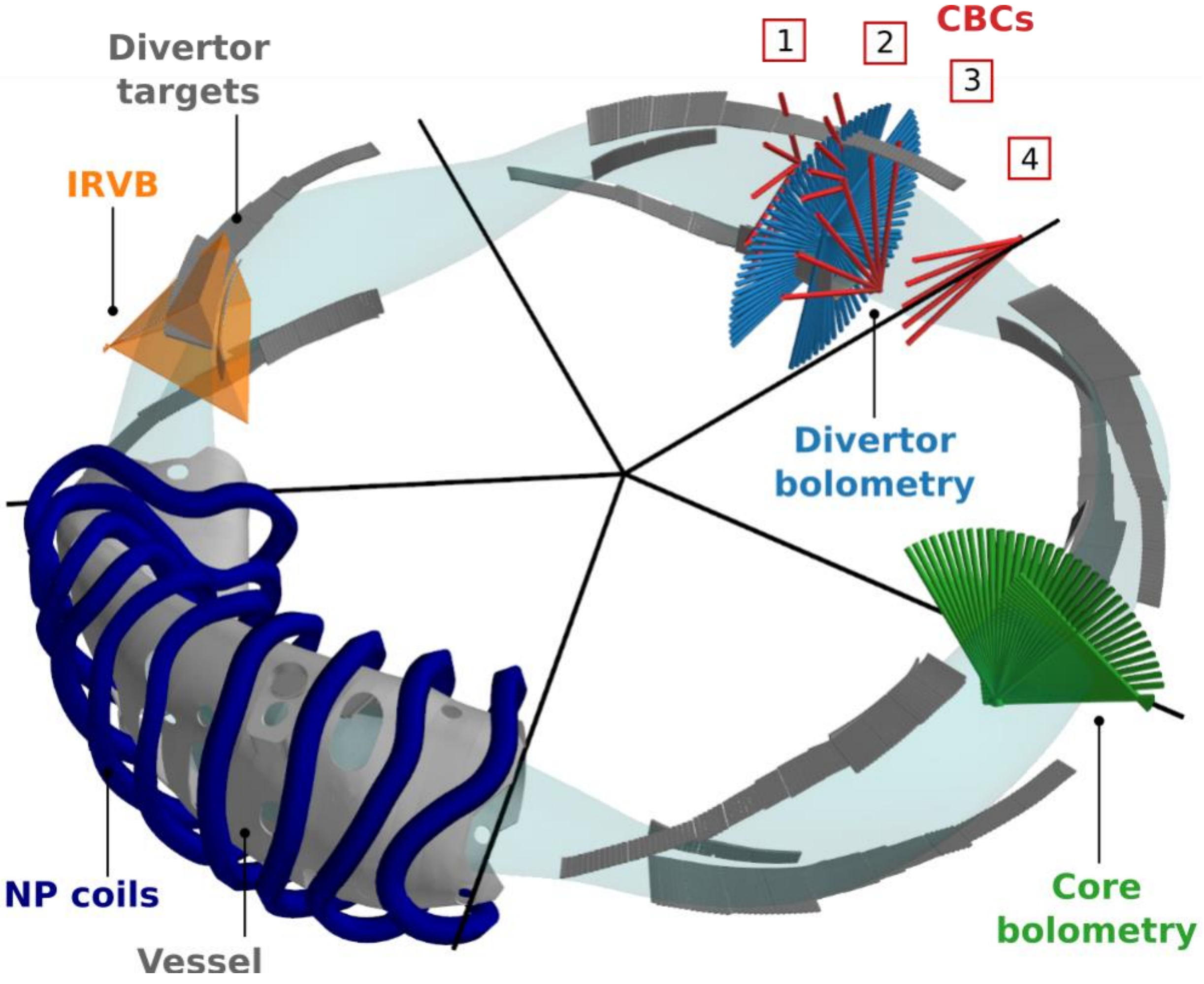

G. Partesotti *in preparation*

Core bolometers

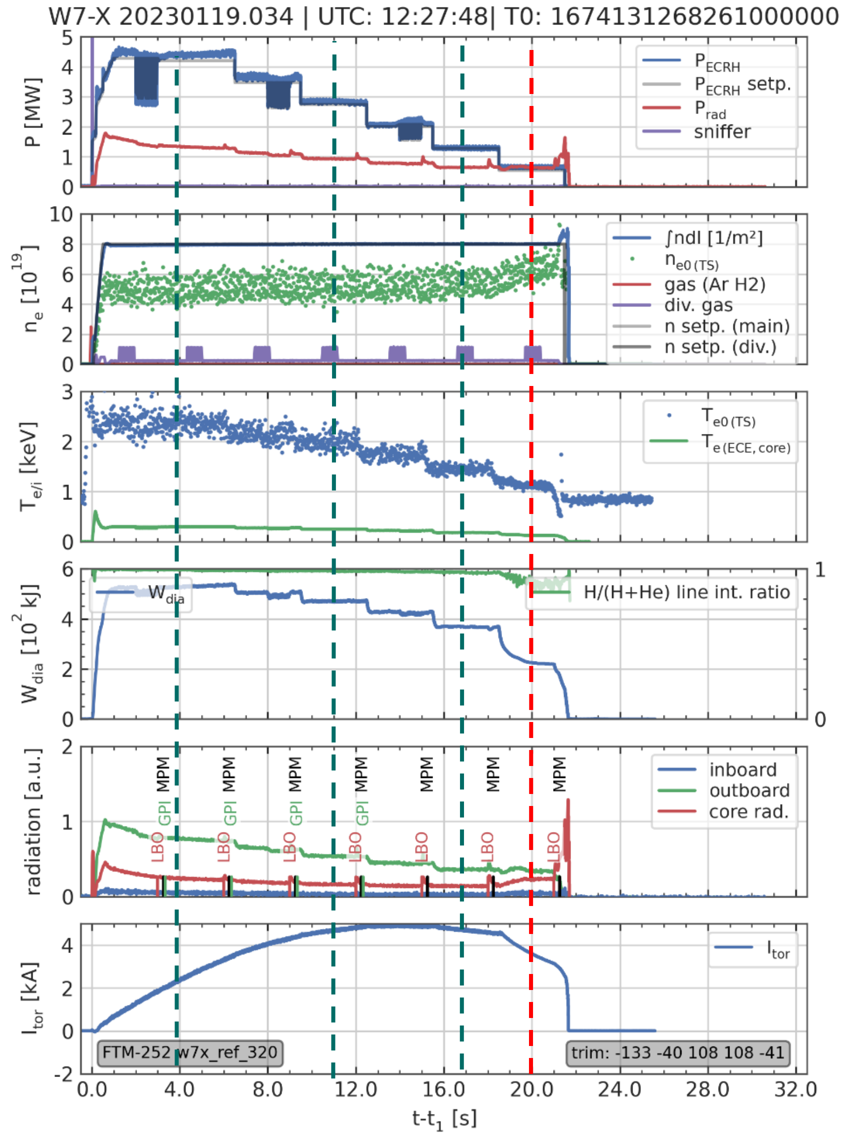

generated Tue Jul 18 19:21:43 2023 - version 3.0 - contact: astechow@ipp.mpg.de - data missing: ['bremsstrahlung', 'XICS_Ti', 'halpha', 'XICS_T

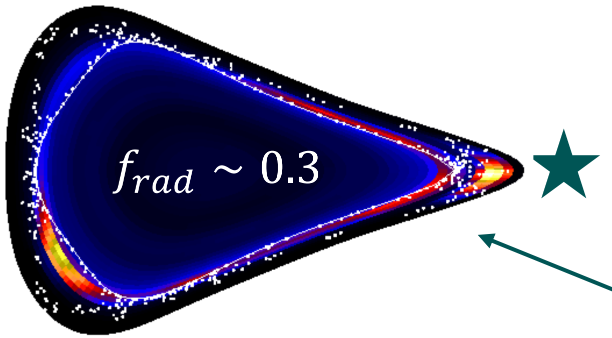

11.0 s, 3.0 MW ECRH, $\varepsilon_{rad,m}$=0.17W/cm^3

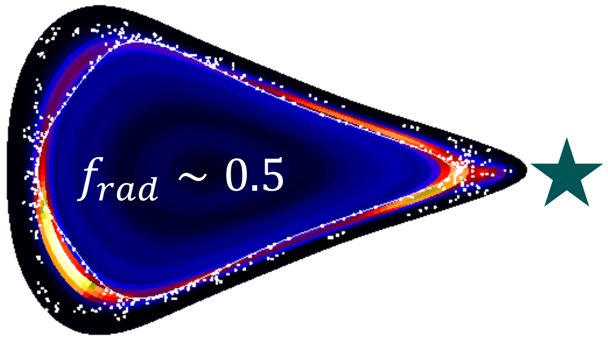

17.0 s, 1.2 MW ECRH, $\varepsilon_{rad,m}$=0.09W/cm^3

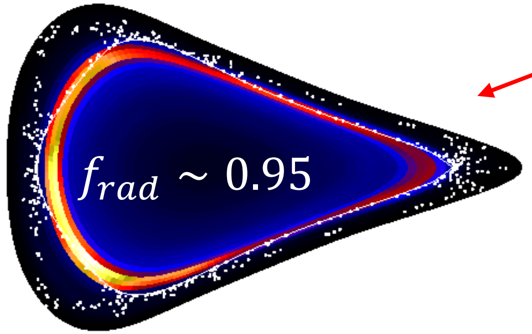

20.0 s, 1.2 MW ECRH, $\varepsilon_{rad,m}$=0.13W/cm^3

High-iota -

courtesy of D. Zhang

- **Attached**
  - **Up-down asymmetry**
  - **Emission at ★ - marked position due to PW interaction**
- **Detached**
  - **In-out asymmetry** with intensive inboard side
  - Emission at ★ disappears

Core bolometers

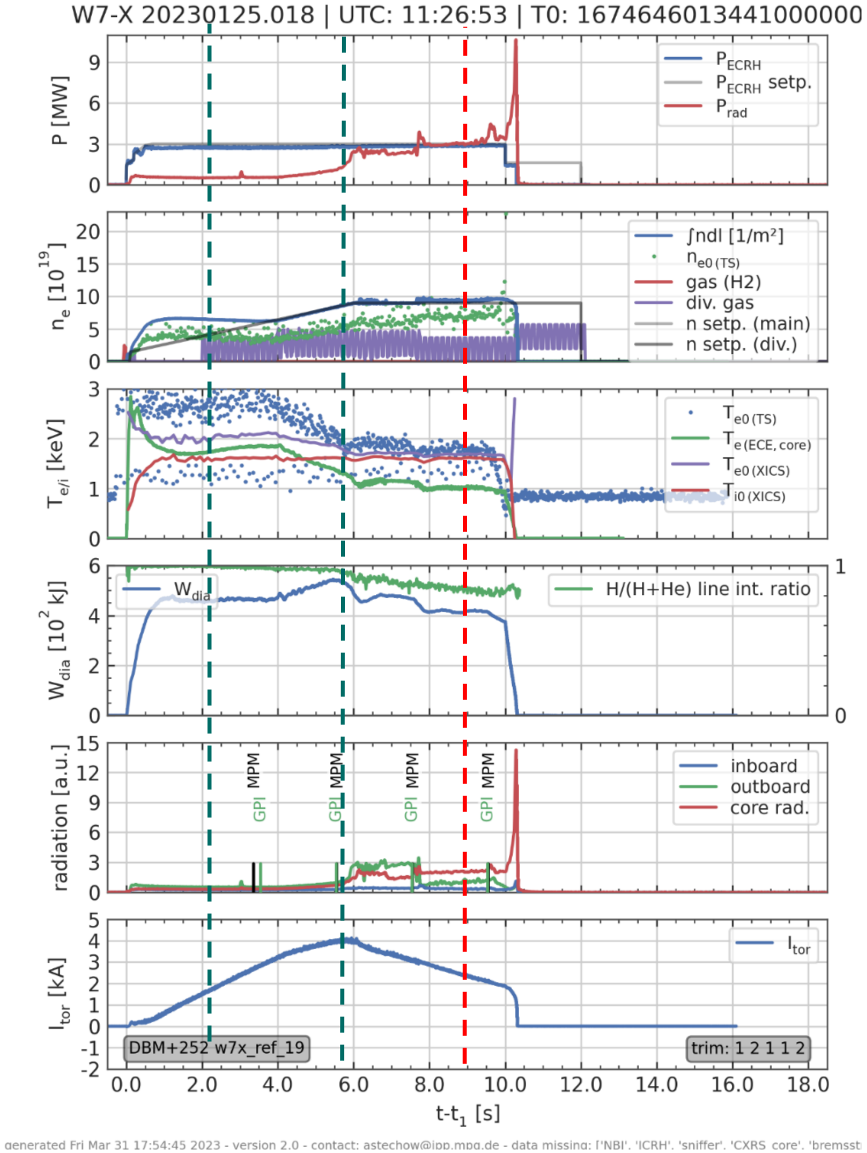

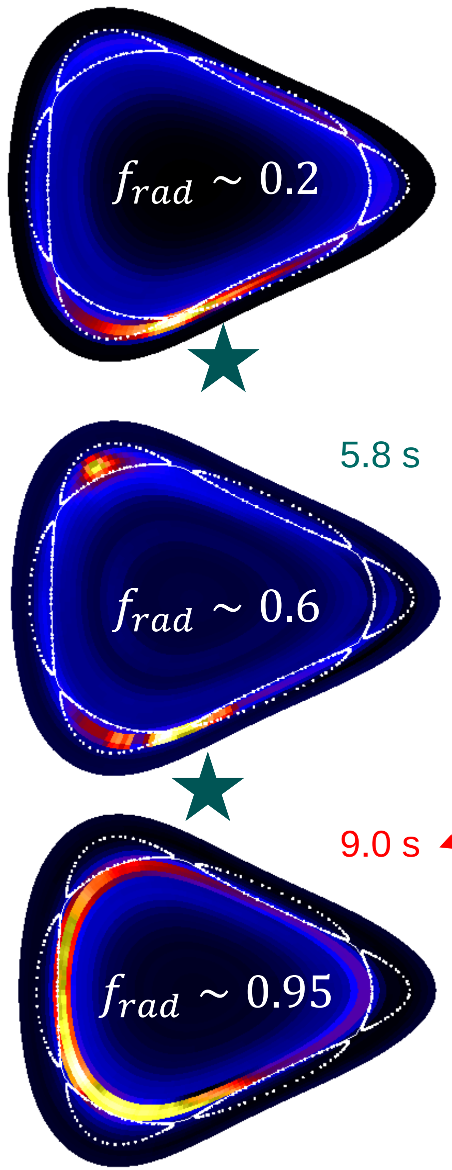

Low-iota +

courtesy of D. Zhang

- **Attached**
  - **Up-down asymmetry**
  - **Strong radiation close to the lower X-point (★ - marked)**
  - Probably due to impurity source (PW interaction)
- **Detached**
  - **In-out asymmetry** (intensive radiation at the inboard side)
  - Emission at ★ disappears

Core bolometers

dominant lower side | dominant upper side

courtesy of D. Zhang	standard (EJM)	low-iota (DBM)	high-iota (FTM)	high-mirror (KKM)
Forward B	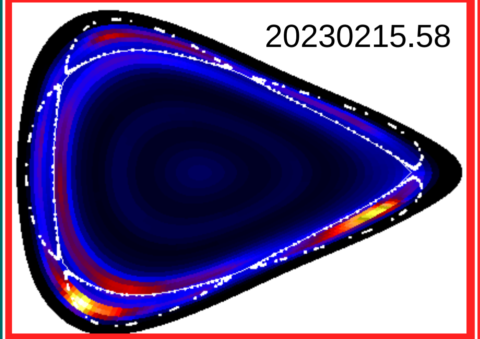	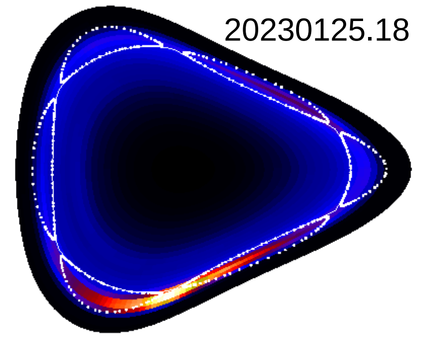	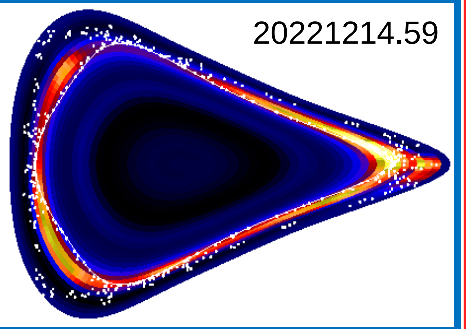	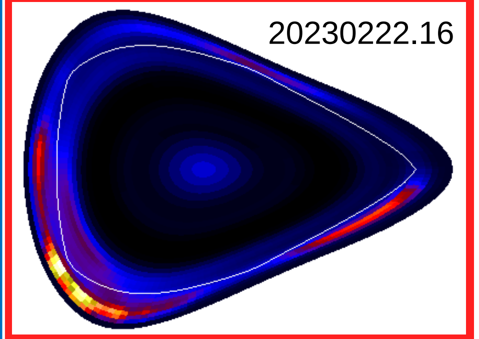
Reversed B	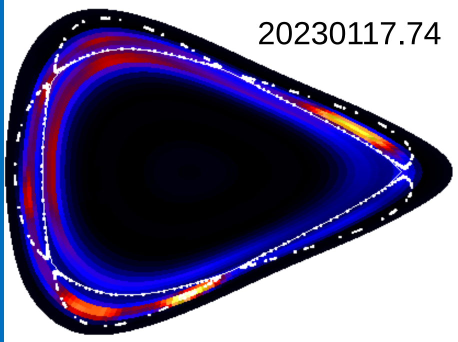	×	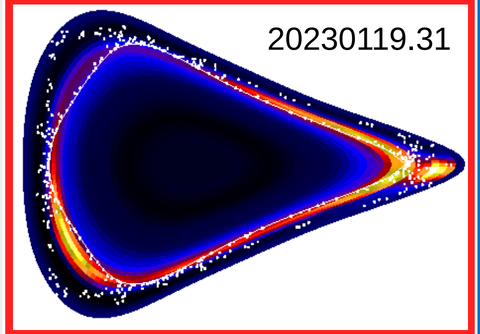	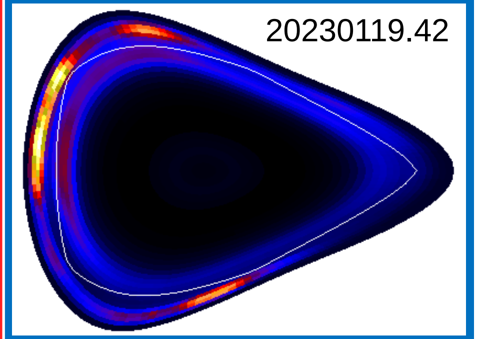
f_{rad}	0.2	0.2	0.3	0.25

Divertor bolometers

Divertor bolometers

[module 40]

Divertor bolometry

Divertor camera

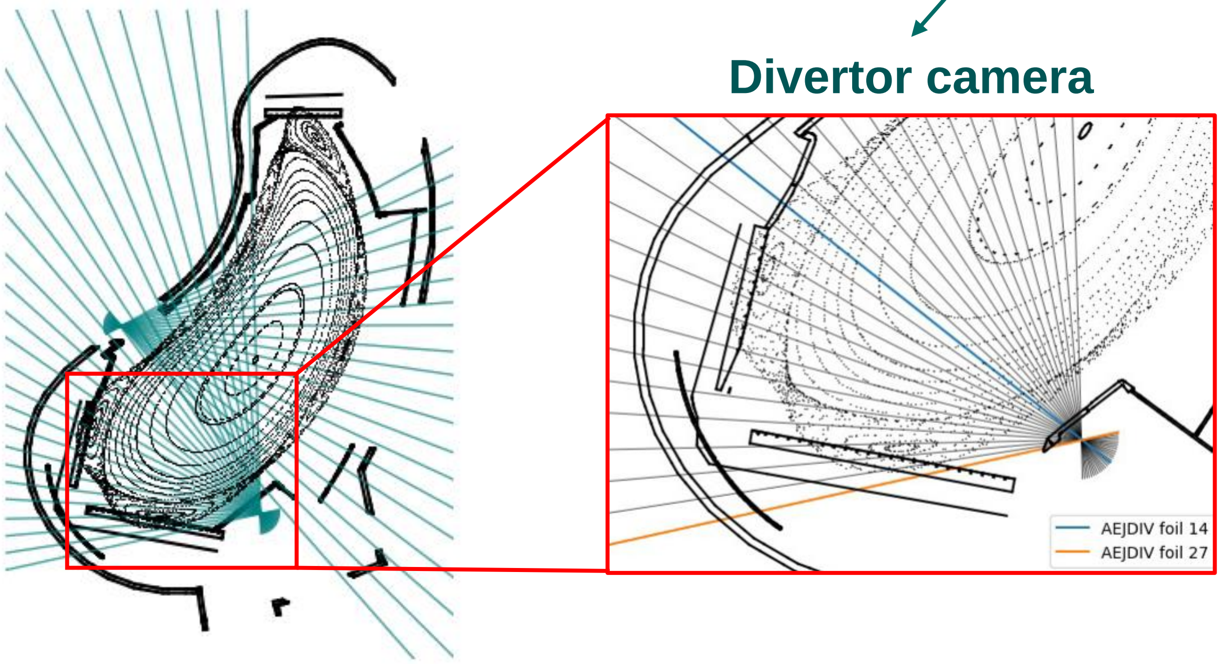

Available lines-of-sight: 32/88 (36%)

Divertor bolometers

Divertor bolometers

[module 40]

Divertor bolometry

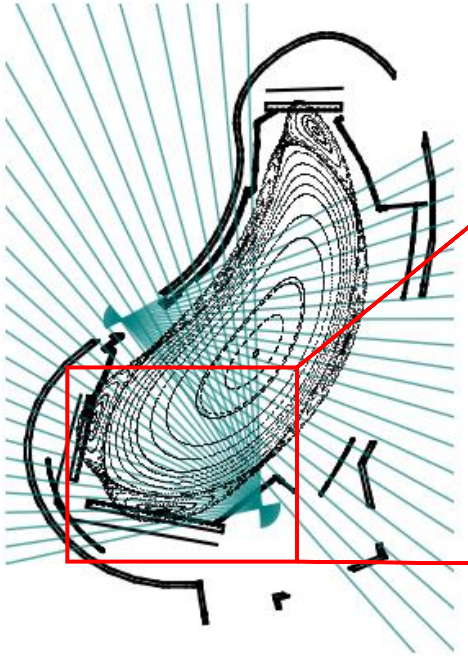

Divertor camera

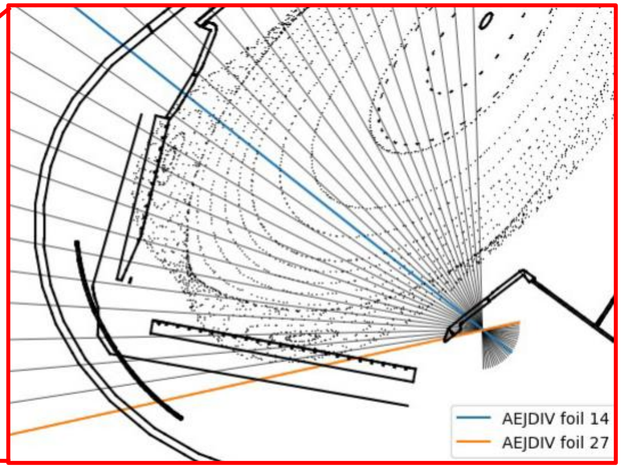

Imaged area

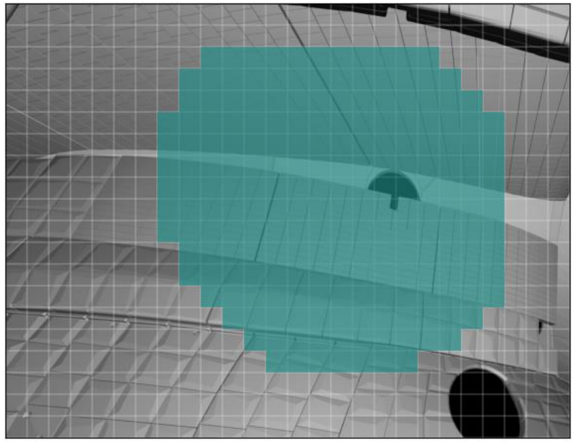

[module 51]

IRVB

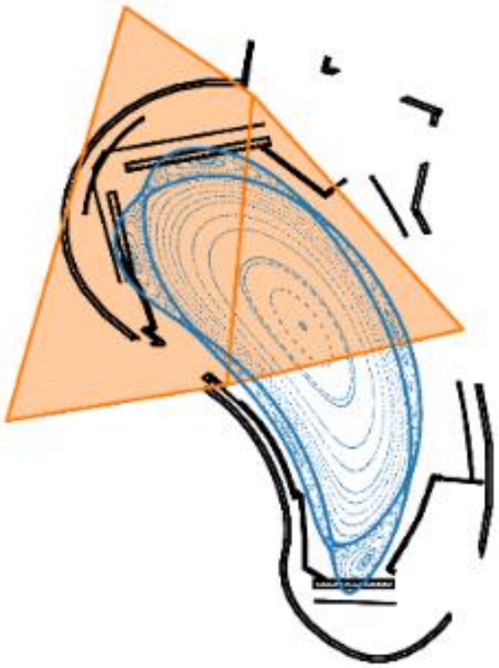

Available lines-of-sight: 32/88 (36%)

Available lines-of-sight: 207/520 (40%)

Divertor bolometers

- IRVB Horizontal direction: toroidal movement
- IRVB Vertical direction: poloidal movement

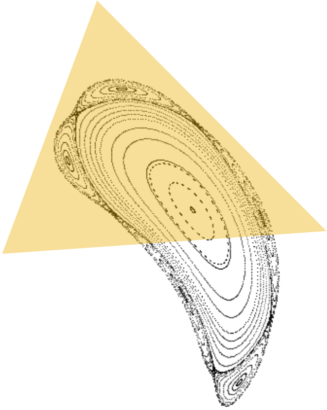

standard

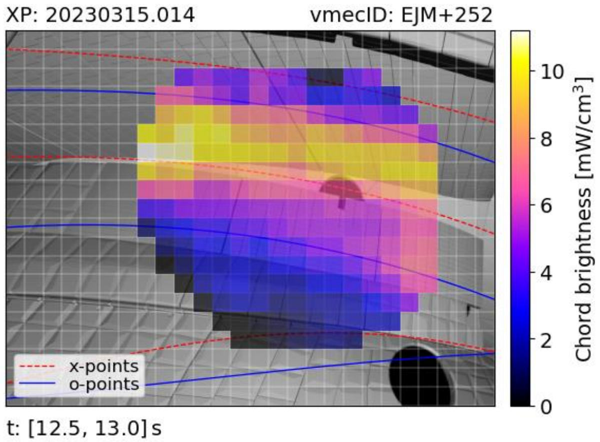

Divertor bolometers

- IRVB Horizontal direction: toroidal movement
- IRVB Vertical direction: poloidal movement
- IRVB observations:
  - **Plasma ε peaking towards $\varphi = 4°$ (in standard)**

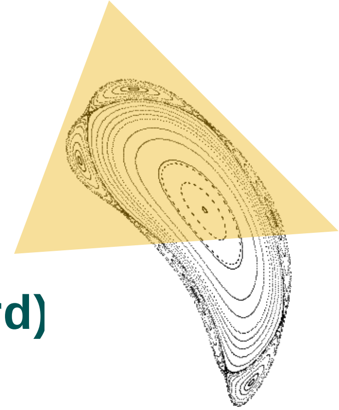

standard

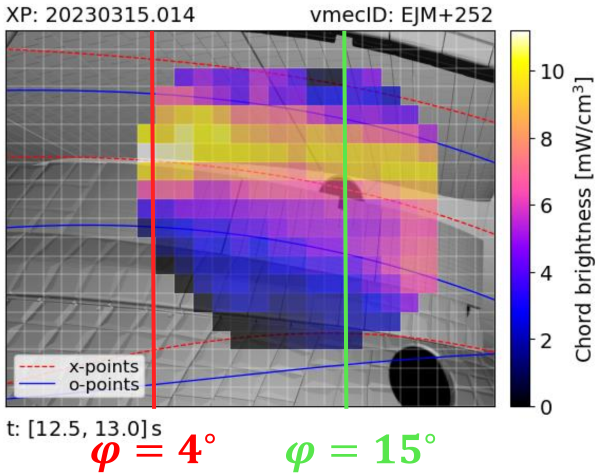

Divertor bolometers

- IRVB Horizontal direction: toroidal movement
- IRVB Vertical direction: poloidal movement
- IRVB observations:
  - **Plasma ε peaking towards $\varphi = 4^{\circ}$ (in standard)**
  - **Plasma ε dominated by target interaction**

standard

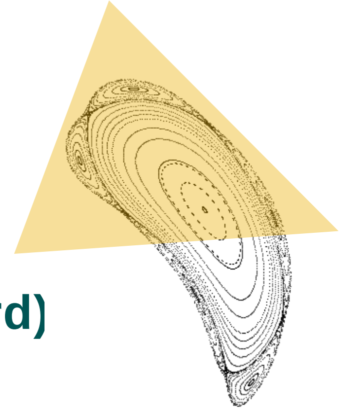

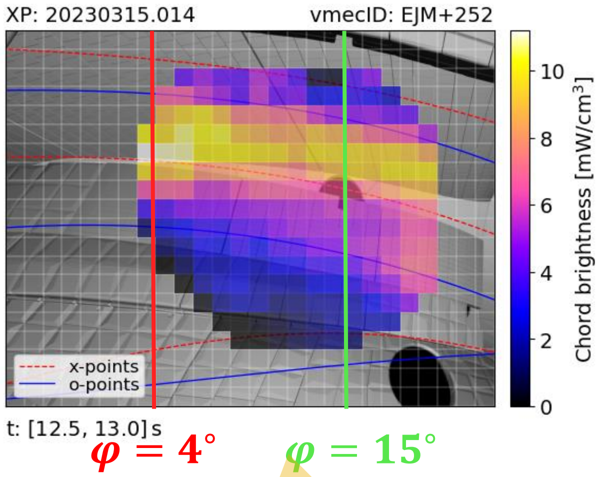

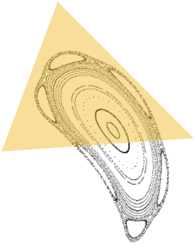

low-iota

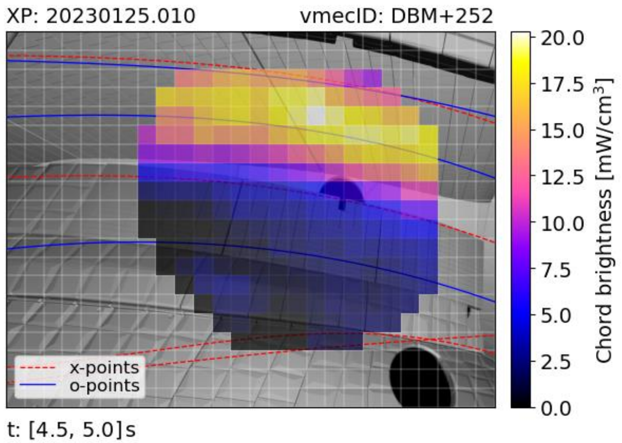

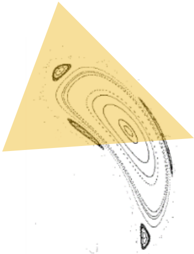

high-iota

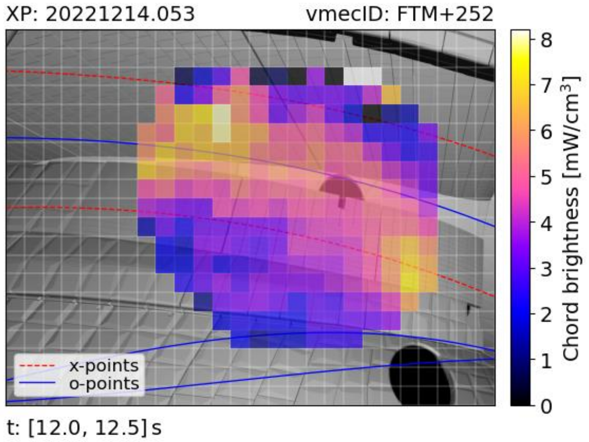

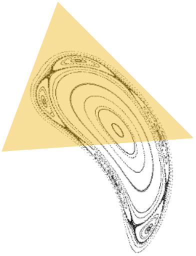

high-mirror

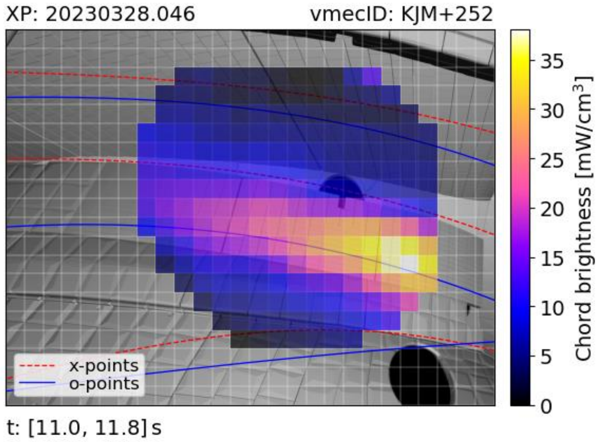

inner islands

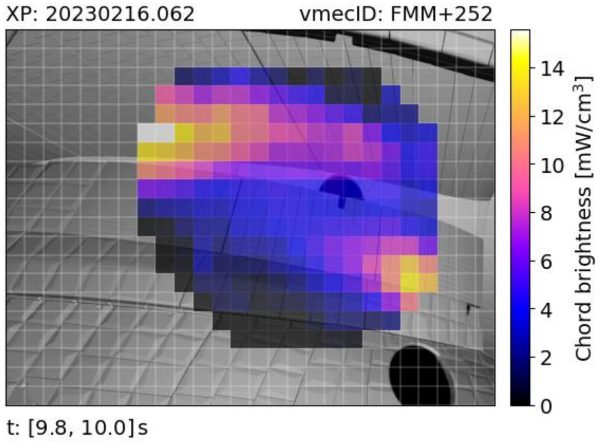

Divertor bolometers

- IRVB does not cover the full poloidal cross section
- **Plasma ε change after field reversal was observed**

standard | **high-mirror** | **high-iota**

forward B / **reversed B**

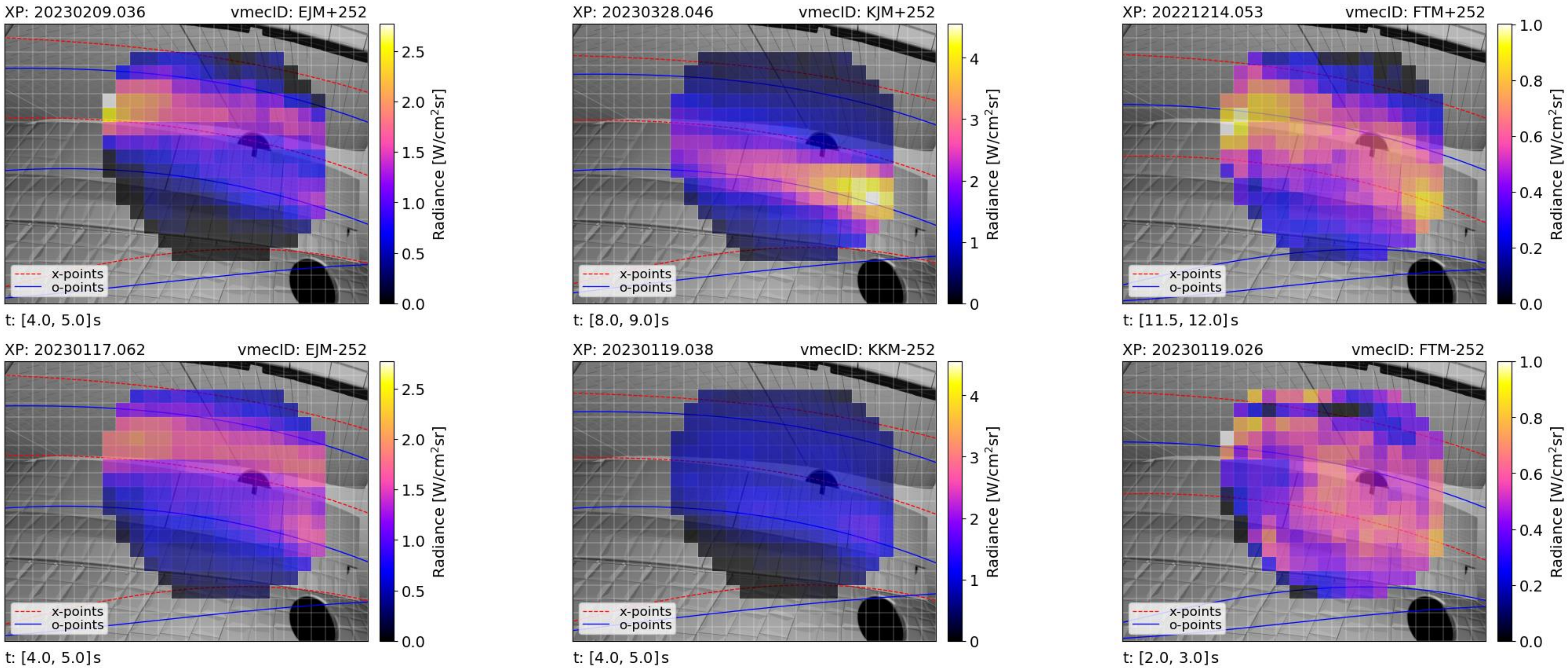

Seeding from upper vs. lower valves

low-iota +

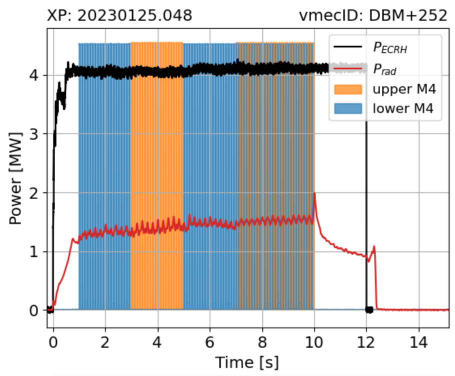

Horizontal bolometer camera

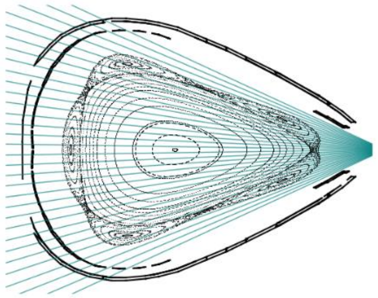

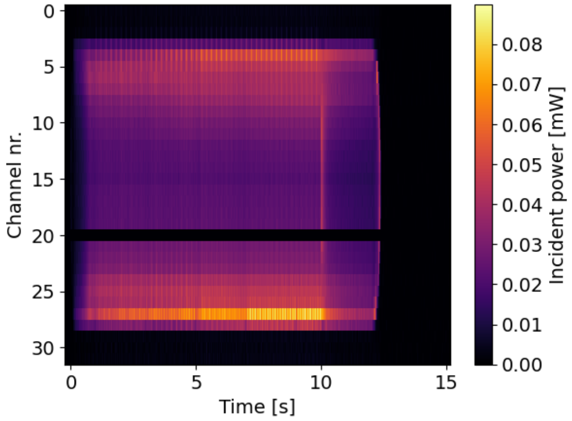

Seeding from upper vs. lower valves

- Higher bolo signal in lower divertor region

  → **Toroidal asymmetry of plasma ε**

- Larger signal step on lower valve injection

  → **Toroidal asymmetry in seeding response**

- Missing standard+ and high-iota

low-iota +

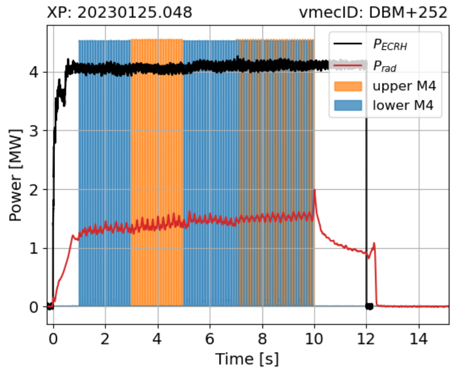

Horizontal bolometer camera

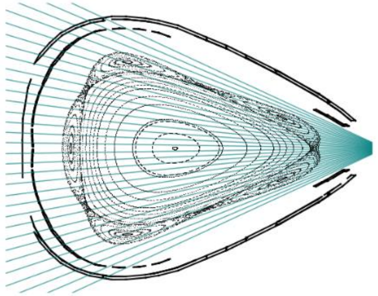

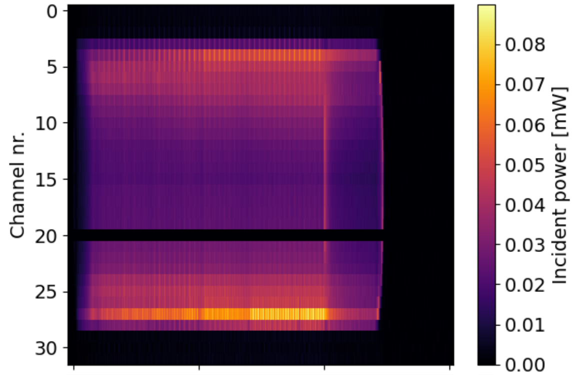

Divertor camera

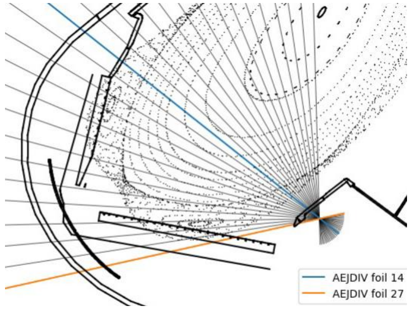

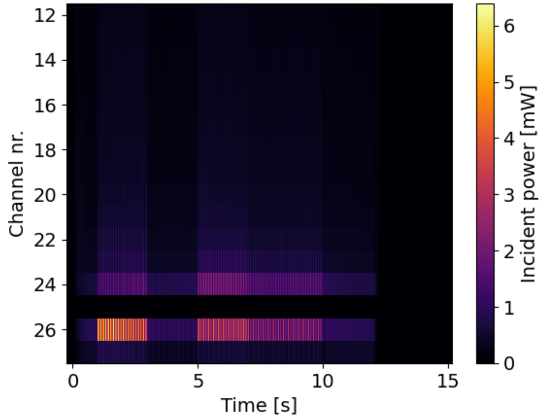

Seeding from upper vs. lower valves

- Higher bolo signal in lower divertor region

  → **Toroidal asymmetry of plasma ε**

- Larger signal step on lower valve injection

  → **Toroidal asymmetry in seeding response**

- Missing standard+ and high-iota

Horizontal bolometer camera

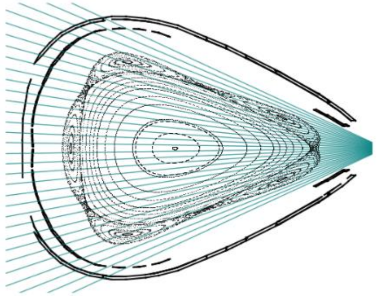

Is the P_{rad} response to seeding asymmetric?

- Different gas pressures used
- Valve calibration is necessary

Divertor camera

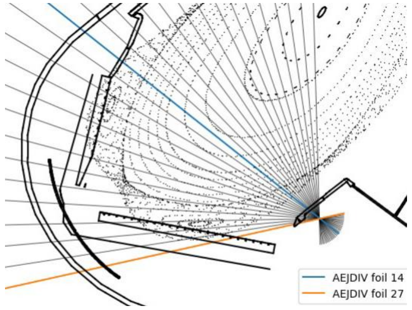

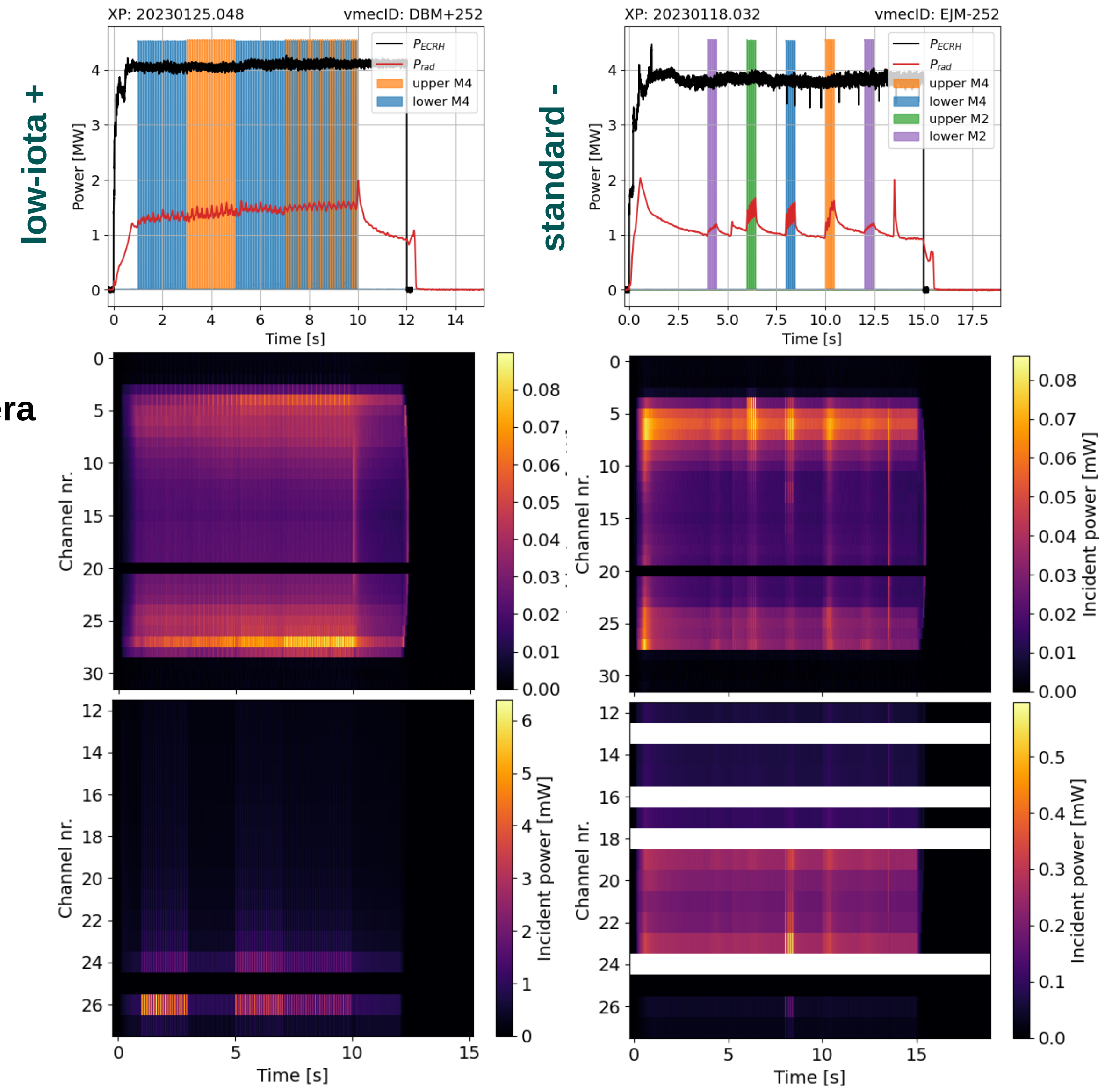

Gas valve calibration

- **Seeding rate is different for upper M2 and lower M2 valves**

  → valve-dependent calibration factor must be used
- However: missing calibration data for full comparison

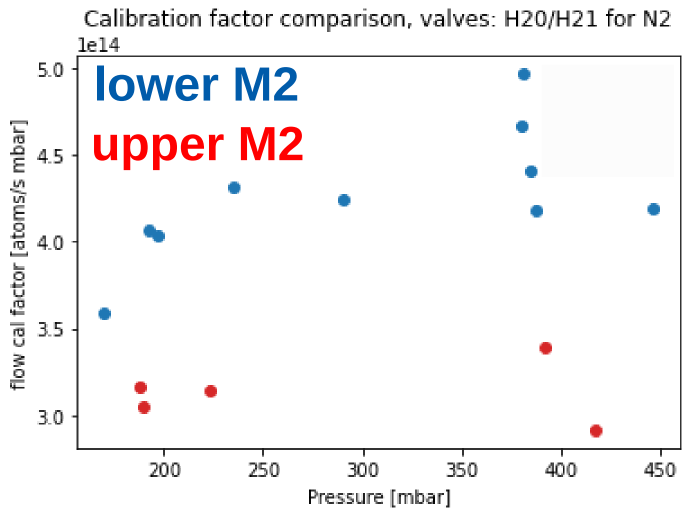

courtesy of A. Tsikouras

Gas valve calibration

- **Seeding rate is different for upper M2 and lower M2 valves**
  → valve-dependent calibration factor must be used
- However: missing calibration data for full comparison
- **Seeding response asymmetry might be present** (in low-iota)
- Must avoid: NBI blips, n_e ramps, different gas pressures …
- **Broader analysis is still missing**
- Valve calibration is ongoing (A. Tsikouras)

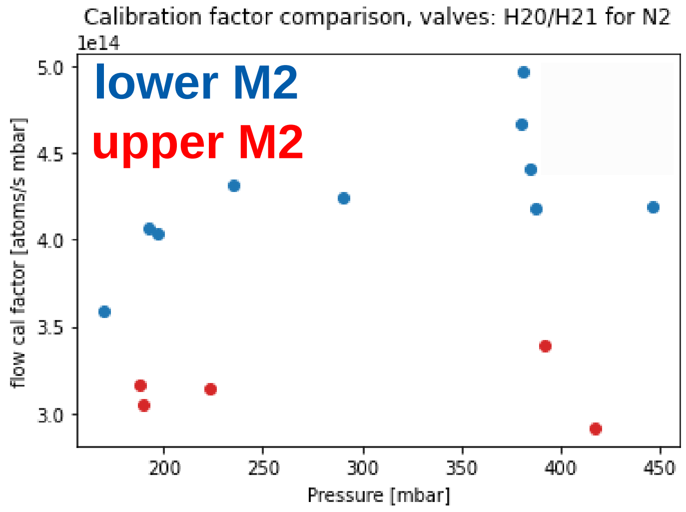

courtesy of A. Tsikouras

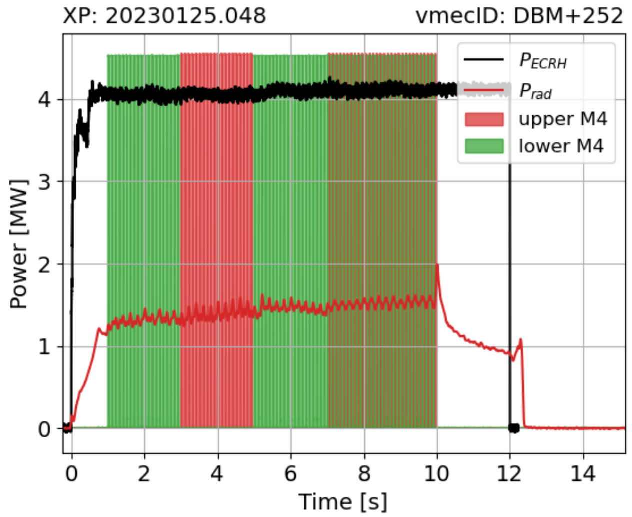

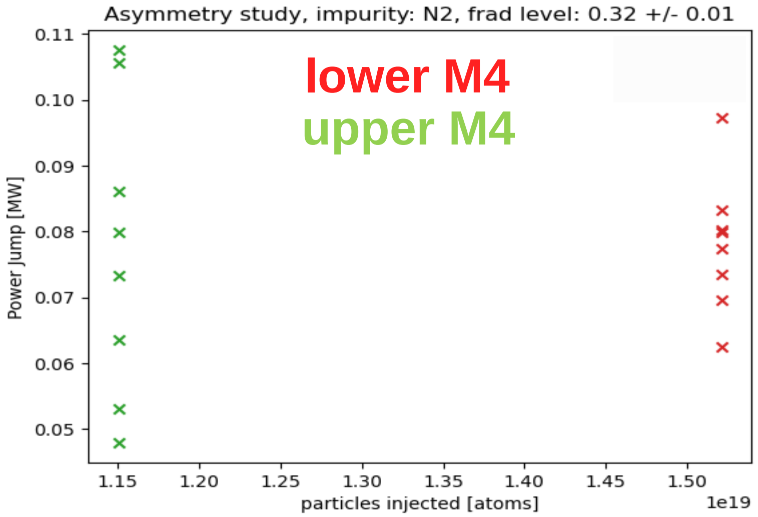

Summary

	Poloidal	Toroidal
Intrinsic	• **Possible explanation with $\boldsymbol{E \times B}$ drifts** • Core system ★ **up-down asymmetry** in attached (reversed in high-iota, stronger in low-iota) ★ **PW interaction in low/high-iota** ★ **in-out asymmetry** in deep detached • IRVB ★ **reversal effects** (different from core system)	• **From asymmetric target interaction** • IRVB ★ **target interaction is dominant** ★ peaking of plasma ε at $\varphi = 4°$matches EMC3-EIRENE results • Divertor system ★ **higher $\boldsymbol{\varepsilon}$ compared to core**
From seeding	• **Possibly due to drifts** • Valves ★ maybe observed in one program (**unclear**)	• **Possibly due to drifts** • Divertor system ★ **localized seeding $\boldsymbol{\varepsilon}$ response**

Proposals

Proposal	Author	Title	Completed	Carried to OP2.2
aalso_004	Arthuro Alonso	Post-pellet seismology for diagnosing impurity collisionality and density asymmetry	**No**	**Yes**
daz_008	Daihong Zhang	Dependence of X-point radiation asymmetry in the triangular cross section with varied local gas-seeding	**Partially**	**Yes**
daz_009	Daihong Zhang	Diagnostics benchmarking (XMCTS, Bolometry) for pol. radiation asymmetries induced by localized low-Z and high Z impurity injection by TESPEL	**Yes**	**No**
daz_010	Daihong Zhang	X-point radiation asymmetry in varied magnetic configurations and reversed field directions	**Partially**	**Yes**
suma_009	Suguru Masuzaki	Up-down asymmetry of divertor particle and heat load in H/He discharges in W7-X		
flr_005	Byron J. Peterson	Effect of impurity seeding on divertor detachment and resulting toroidal and poloidal asymmetries	**Partially**	**Yes**
glp_001	Gabriele Partesotti	Localized impurity seeding for toroidal and poloidal radiation asymmetries	**Partially**	**Yes**

Proposals (OP2.2)

- **Intrinsic asymmetries**
  - More forward/reversed programs
  - DBM- missing

- **Asymmetries due to seeding**
  - Calibration of valve performances with one gas (N_2?)
  - Load same gas in all valves (N_2?)
  - Missing seeding in some magnetic configurations
  - Avoid: NBI blips, n_e ramps, different gas pressures

- **IRVB and Divertor bolometry will be 100% operational + CBCs**
  - Divertor tomography
  - Toroidal distribution of plasma $\boldsymbol{\varepsilon}$

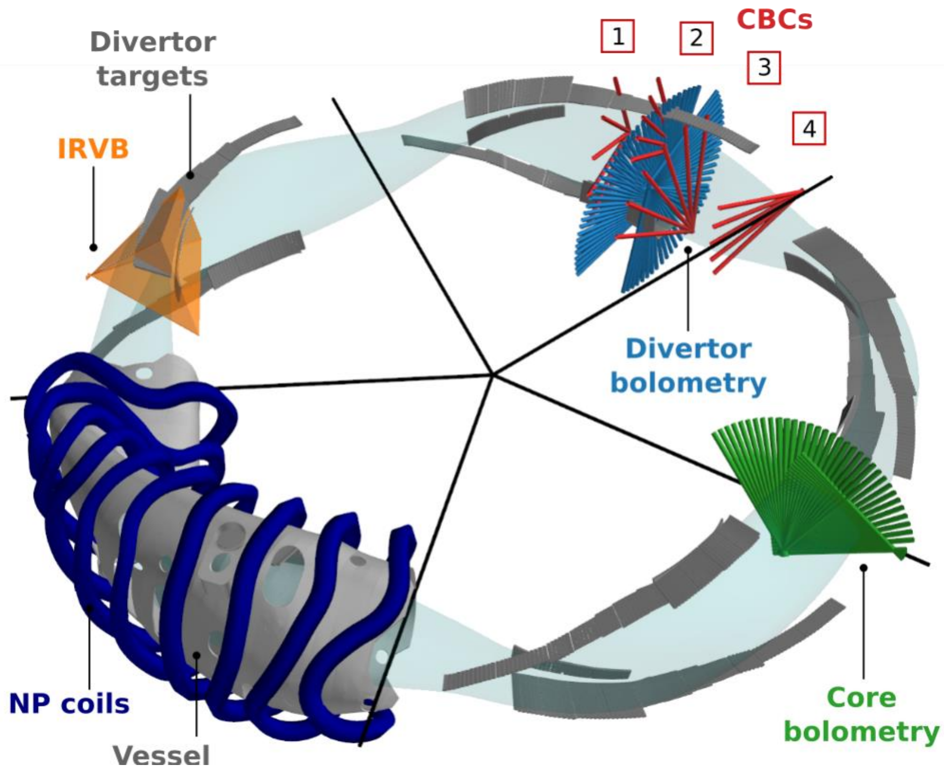

G. Partesotti *in preparation*

Thank you for your attention!

Additional slides

Outline

- **Introduction**
  - Poloidal asymmetry
  - Toroidal asymmetry
- **Intrinsic asymmetries**
  - Core bolometers
  - Divertor bolometers
- **Asymmetries due to seeding**
  - Seeding from upper vs. lower valves
  - Gas valve calibration
- **Summary**
- **Proposals**

IRVB signal and target interaction

- **IRVB view:**
  - Horizontal direction: toroidal movement
  - Vertical direction: poloidal movement
- IRVB observations:
  - **Plasma ε peaking towards $\varphi = 4°$**
  - **Plasma ε dominated by target interaction**

low-iota | **standard** | **high-iota**

IRVB measurement

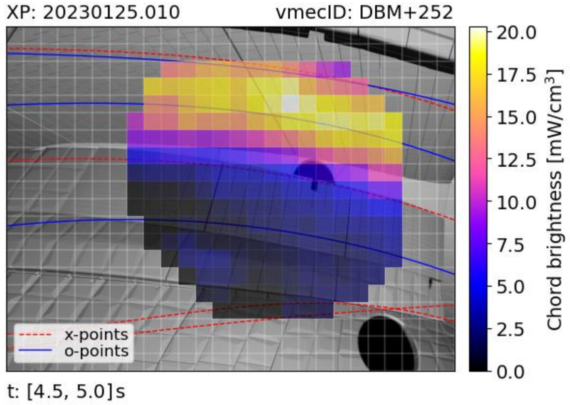

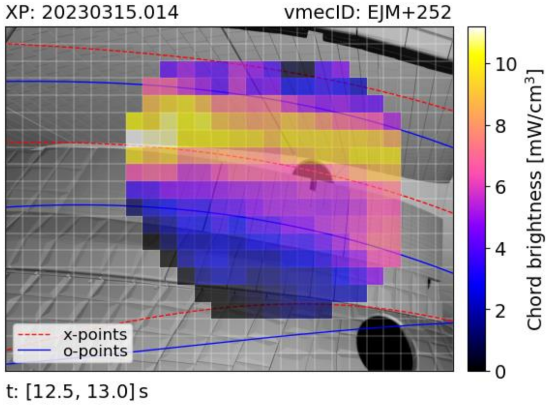

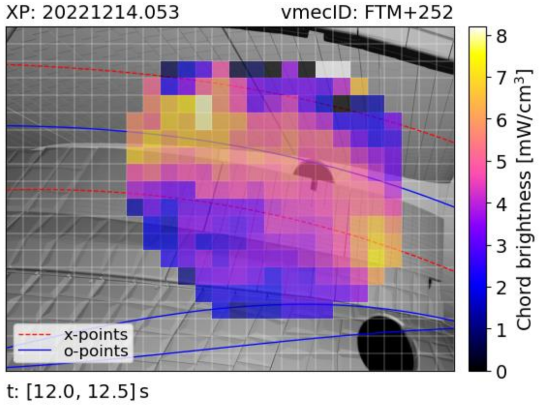

Divertor temperature

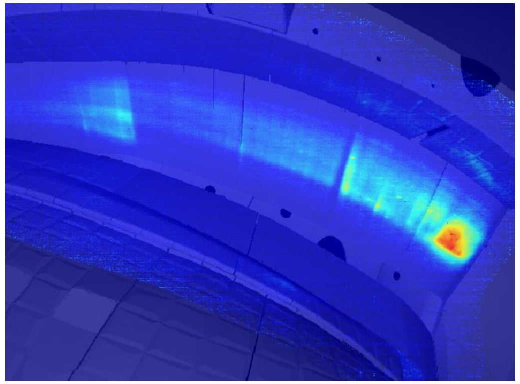

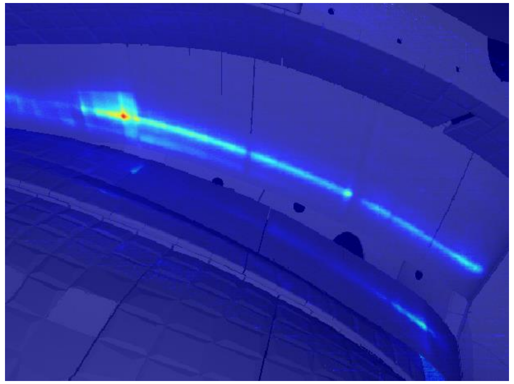

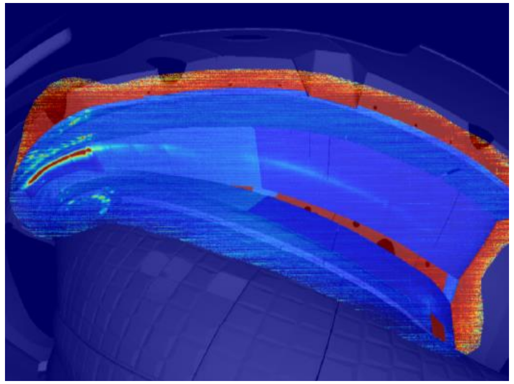

Poloidal asymmetry

- **Poloidal $E \times B$ drift inside the island**

  $\rightarrow$ Asymmetric island n_e and particle fluxes to targets

  $\rightarrow$ Asymmetric n_e and impurity concentration at the targets

  $\rightarrow$ Asymmetric radiated power density

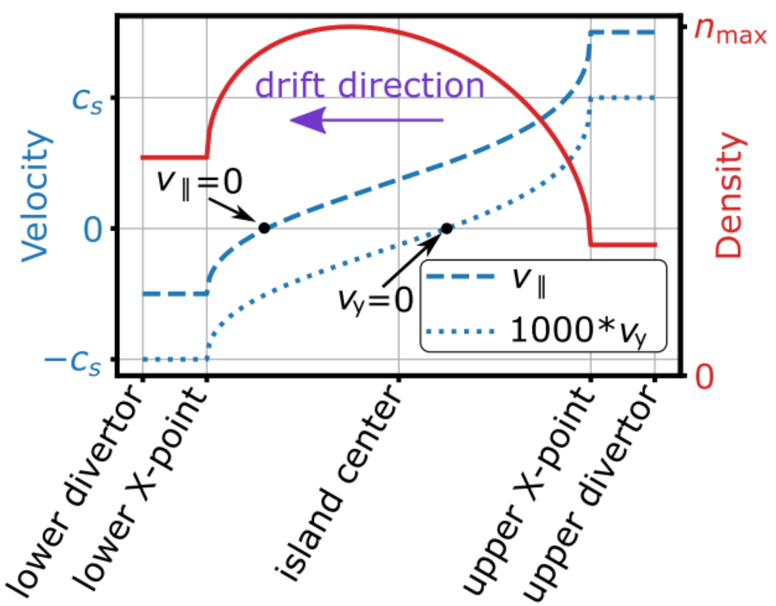

M. Kriete *et al* 2023 *Nucl. Fusion* **63** 026022

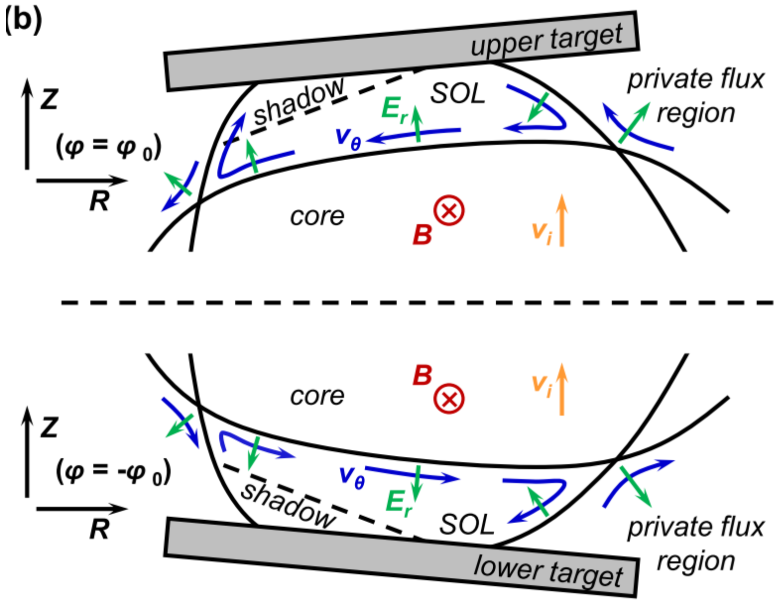

K. C. Hammond *et al* 2019 *Plasma Phys. Control. Fusion* **61** 125001

Carbon imp. rad. asymmetry in “standard” plasma (OP1.2b)

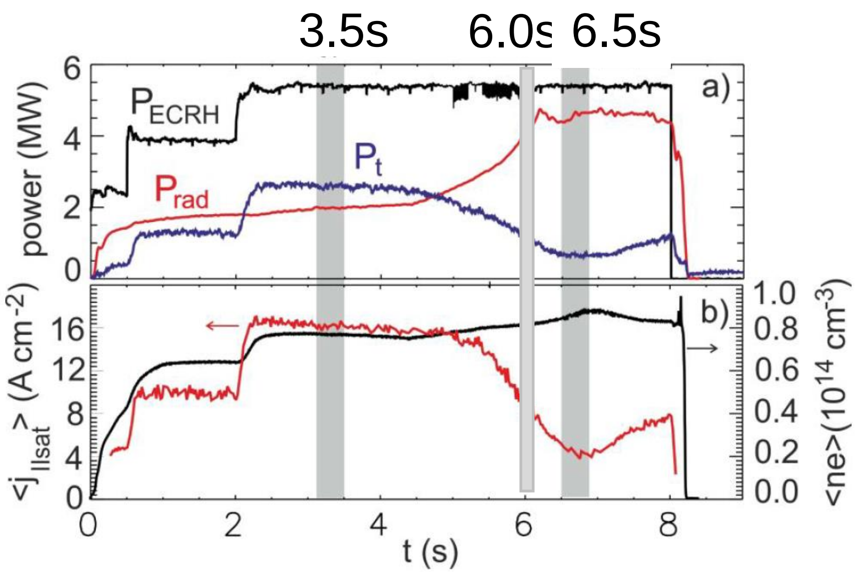

Adopted from [Feng, NF,2021

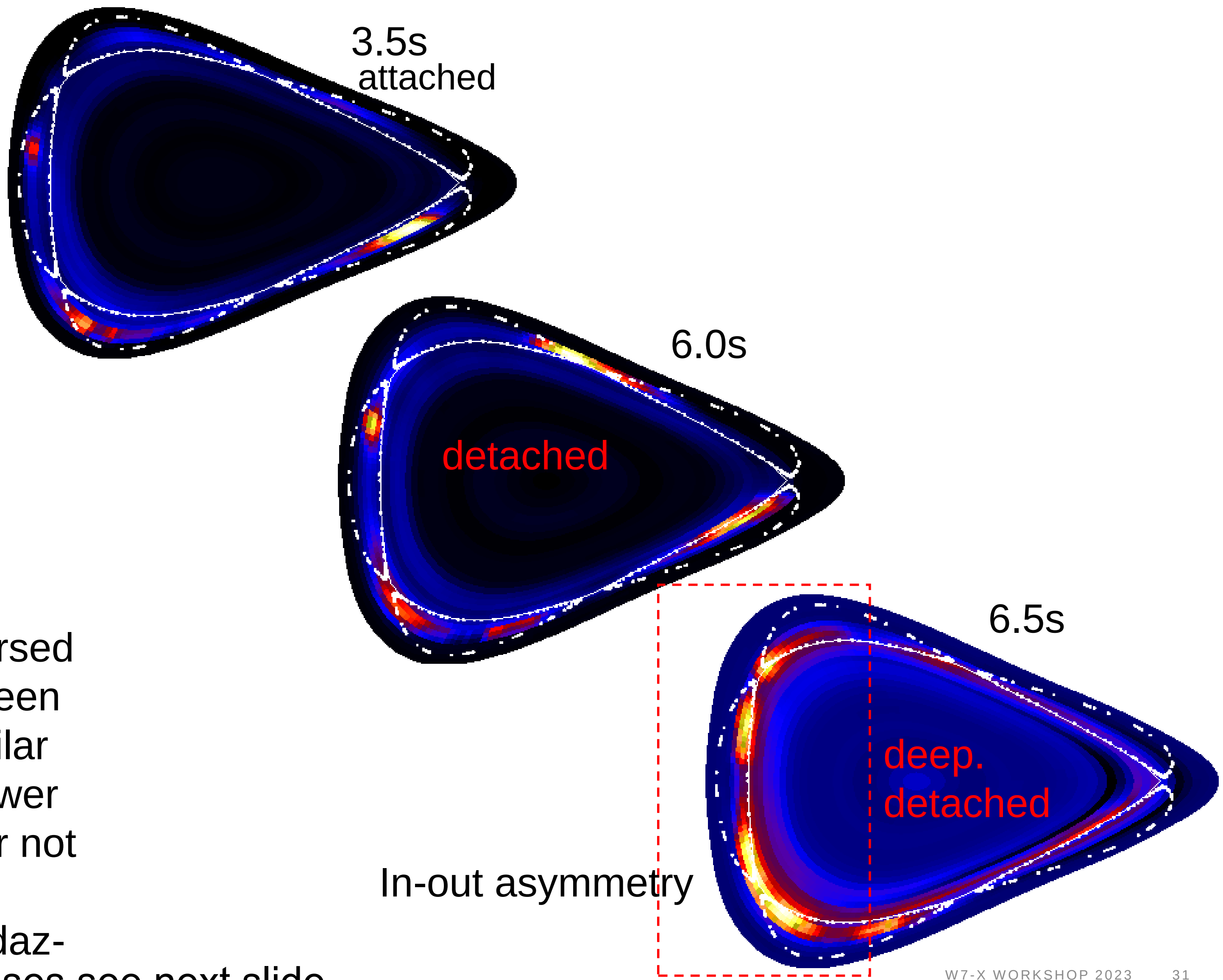

Note:
In OP2.1, experiments in reversed field EJM- configuration has been performed; unfortunately, similar plasma condition with high-power detachment not conducted (or not jet found)
(which might associated with daz-010 proposal)!

Low-power cases see next slide ……

2D rad. distrib. from carbon in “standard” configuration

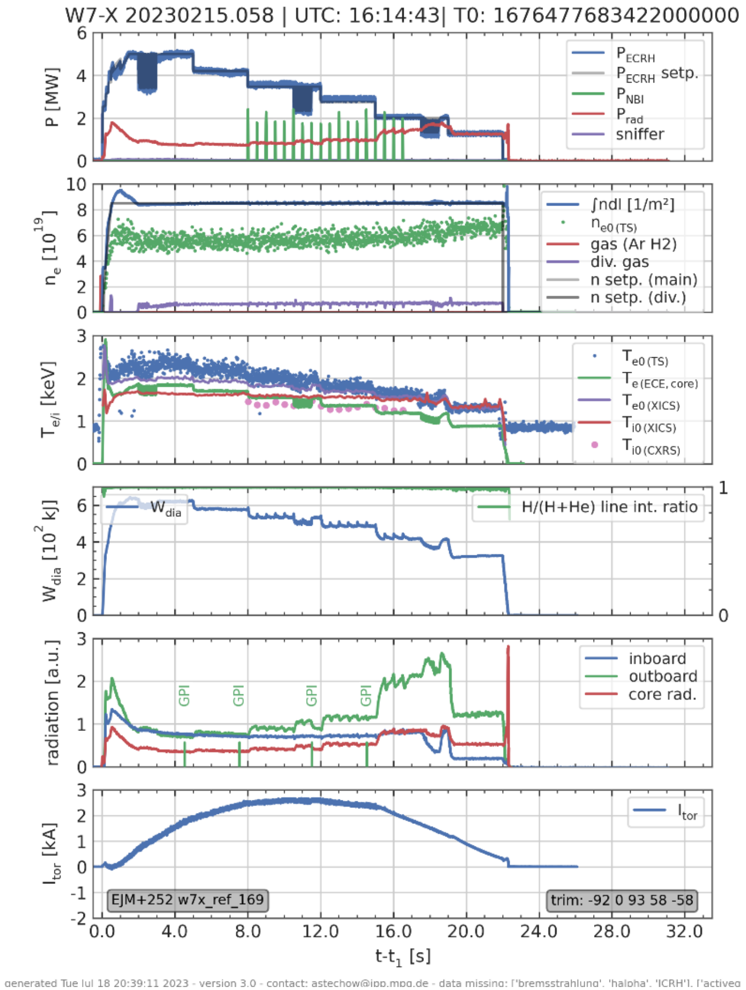

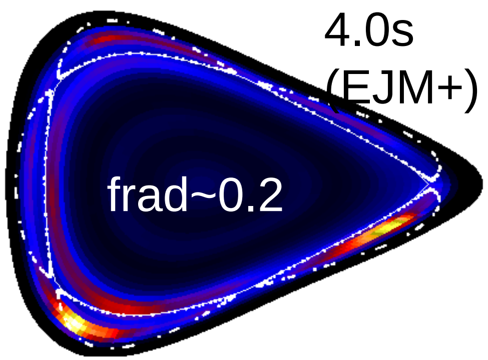

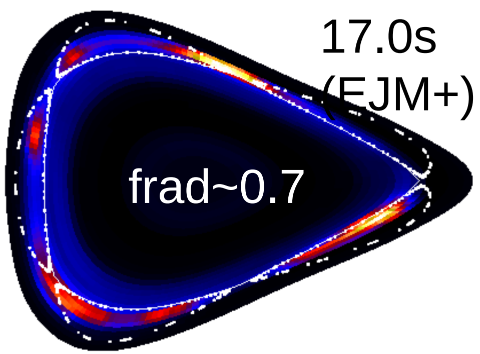

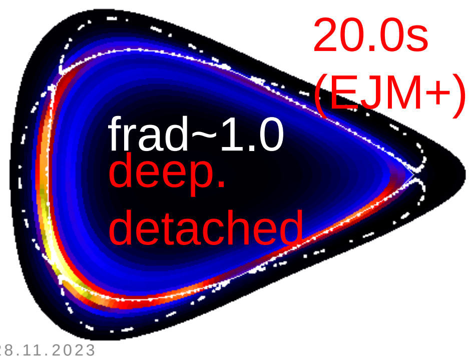

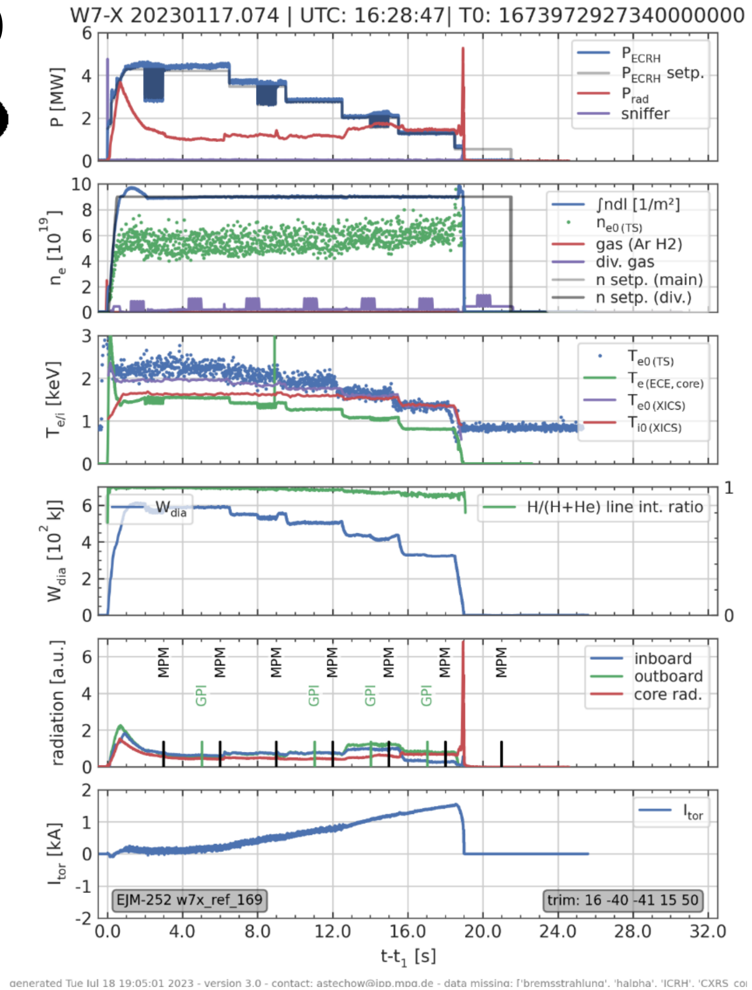

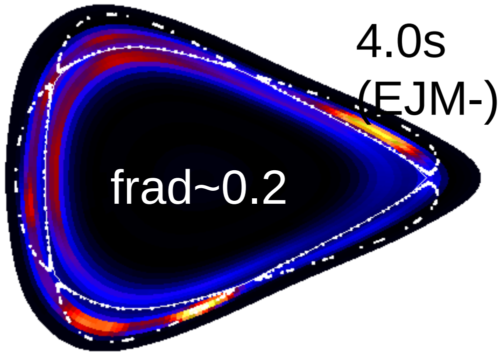

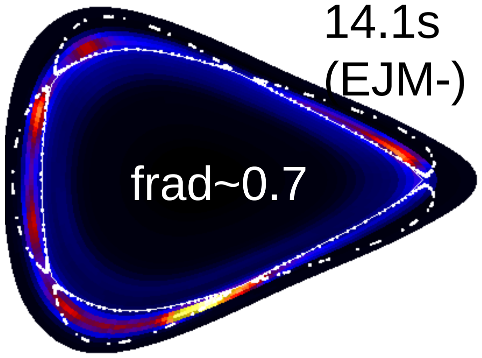

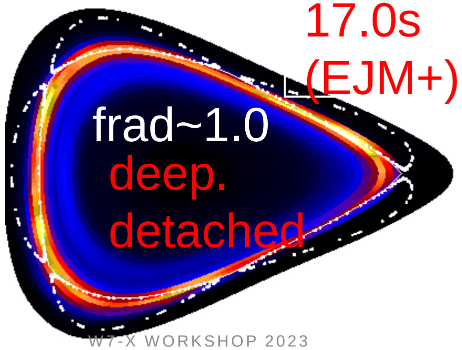

IRVB view

Several bolometry systems at W7-X:

- **Resistive bolometers**
  - [1] Core bolometry (source of P_{rad} signal)
  - Divertor bolometry
  - Compact Bolometer Cameras (CBCs)
- **InfraRed** imaging **Video Bolometer** (IRVB)

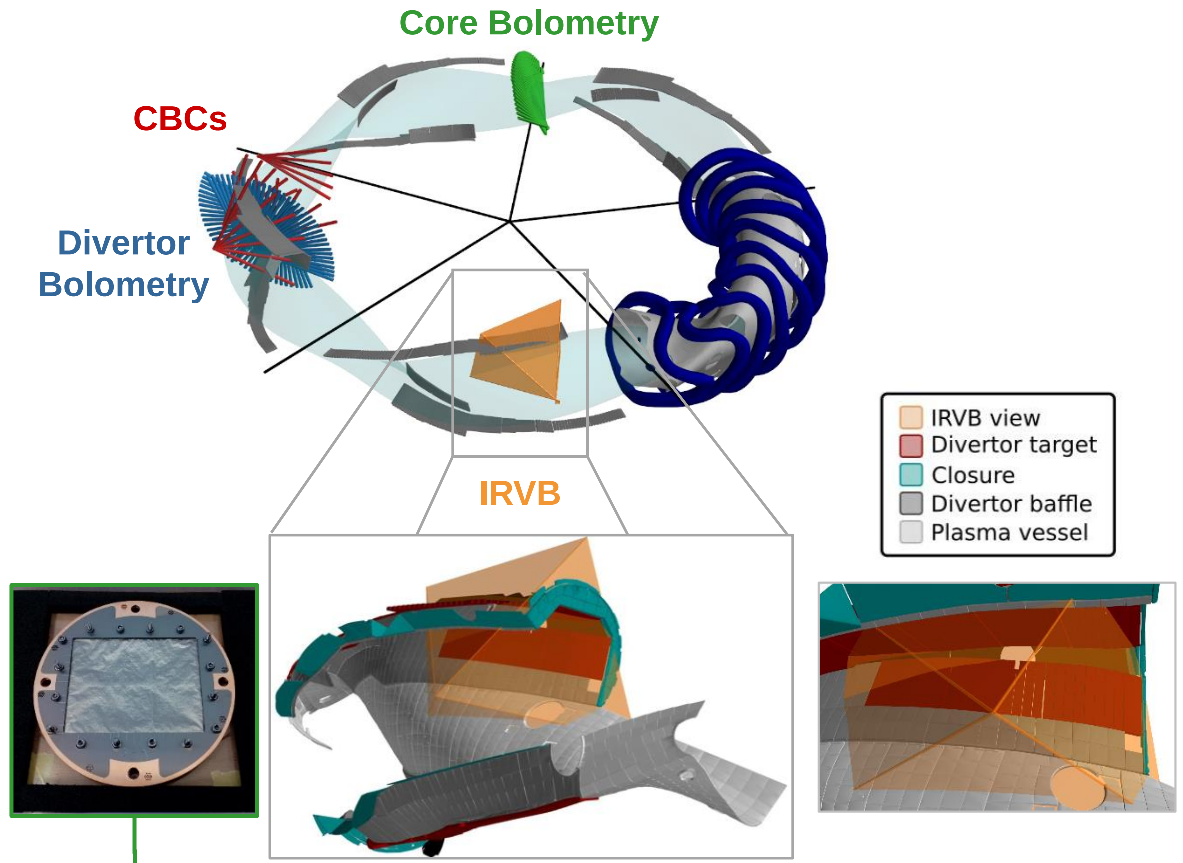

The IRVB diagnostic:

- 7x9 cm C-coated **gold foil** (5 μm thick)
- High-resolution **IR camera**
- **Optical setup** (Au-coated parabolic mirrors)
  - → **cable-free**
- Large number of channels (26x20 = 520)
- No active water cooling

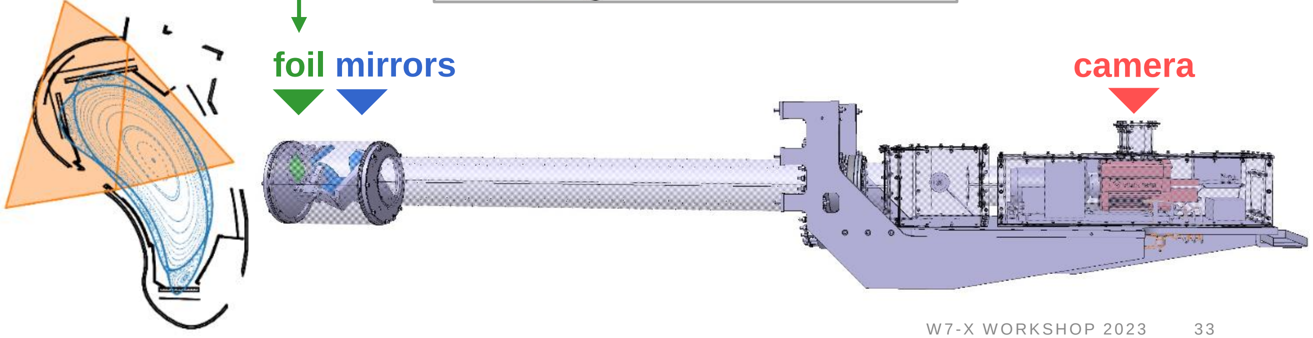

IRVB modeling

1. The **temperature data is mapped** from the IR camera image to the foil pixels
2. The incident radiated power, integrated along each channel line-of-sight P_{lin} is calculated by solving the inverted **2-D heat transfer equation** [1]

$$\frac{dT}{dt} = \underbrace{\boxed{D\left[\frac{d^2T}{dx^2}+\frac{d^2T}{dy^2}\right]}}_{\text{diffusion}} + \underbrace{\boxed{\frac{d}{dt}\left(\frac{P_{lin}}{c}\right)}}_{\text{incident power}} - \underbrace{\boxed{\frac{d}{dt}\left(\frac{\varepsilon\sigma_{SB}\left[T^4-T_{amb}^4\right]}{c}\right)}}_{\text{black-body emission}}$$

3. The incident power P_{lin} is normalized to the channel geometry (pixel etendue e and line-of-sight length d_{LoS}) obtaining the **chord brightness** $P_{chord} = \frac{P_{lin}}{e d_{LoS}}$

T on IR camera

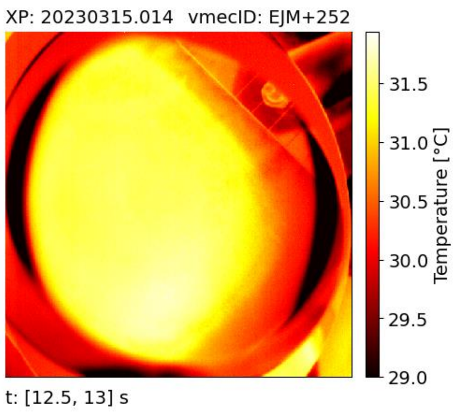

1

T on foil view

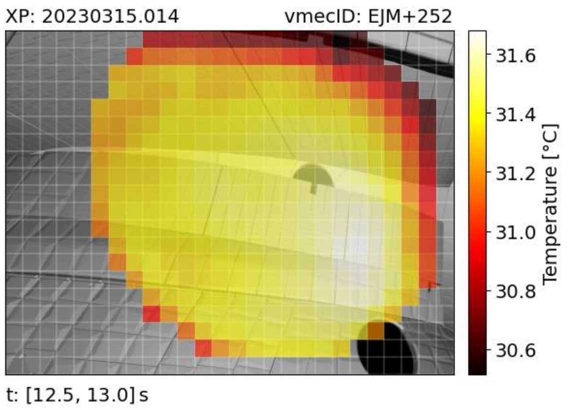

2

P_{lin} on foil view

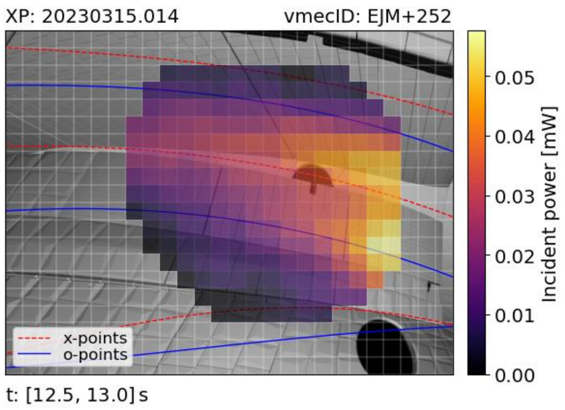

3

P_{chord} on foil view

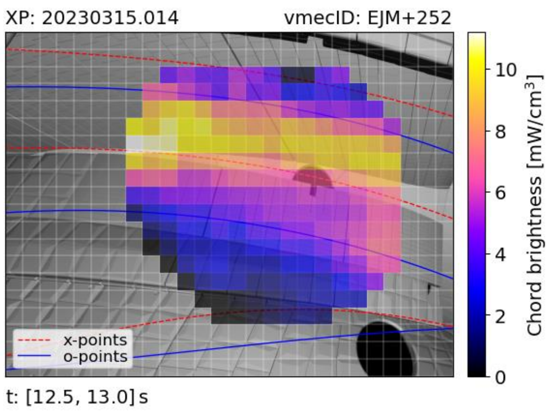

Comparison to EMC3-EIRENE

Experimental and synthetic measurements, calculated with EMC3-EIRENE, are compared for two cases at different radiated power fraction $f_{rad} = \frac{P_{rad}}{P_{heat}}$.

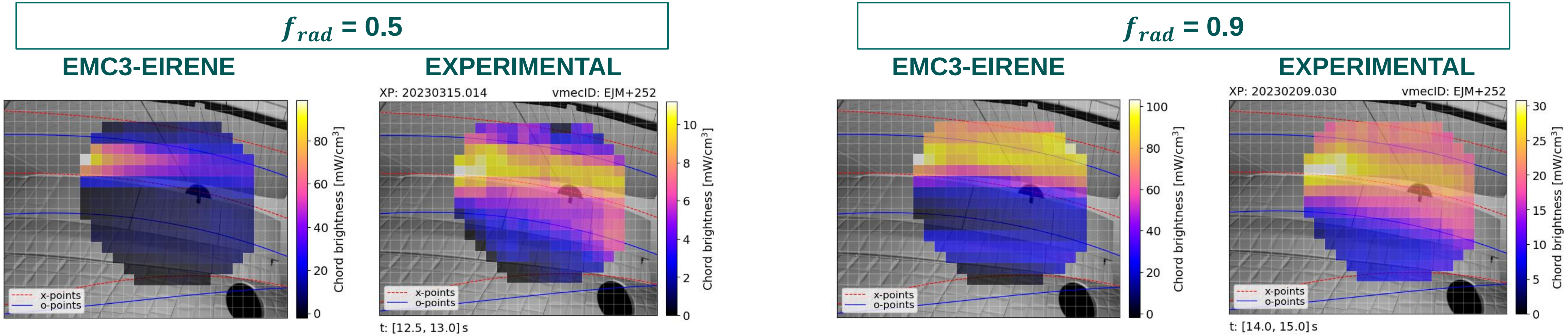

- Comparison is only **qualitative**
- One island contributes to most of the emission
- Radiation peak is aligned on **same island X-/O-point**
- Radiation zone broadens poloidally at high f_{rad}
- Additional experimental noise (vibrations?)
- EMC3-EIRENE doesn't capture **right-hand side emission spots**

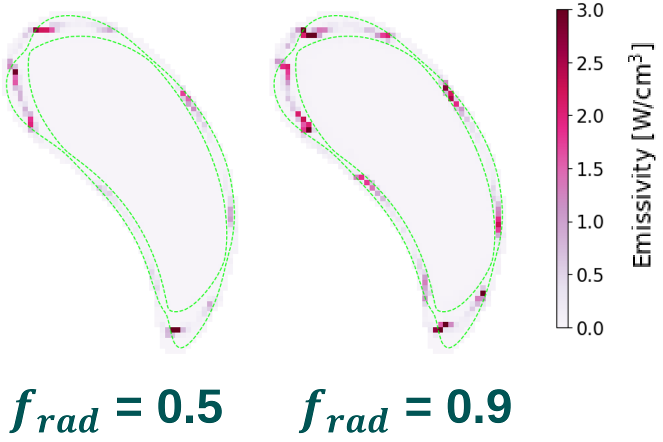

GPT Projections

Projection **Experiment**

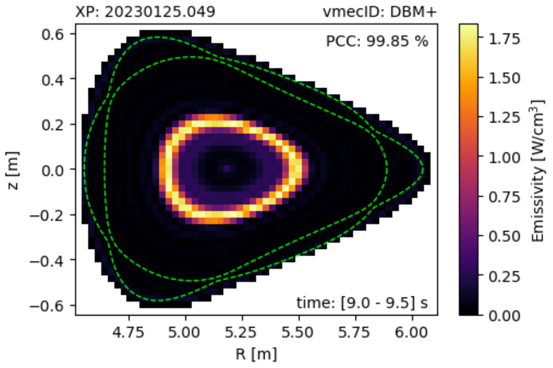

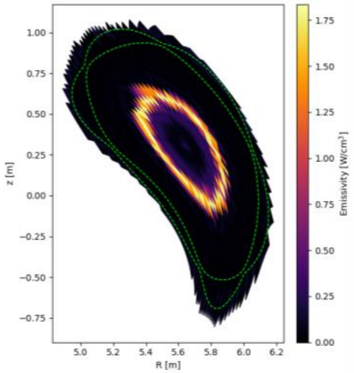

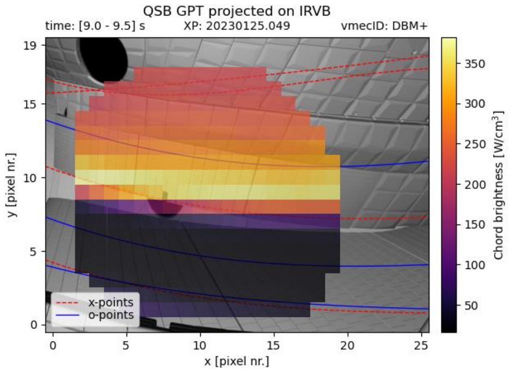

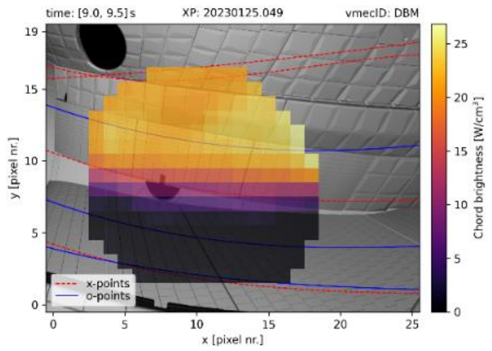

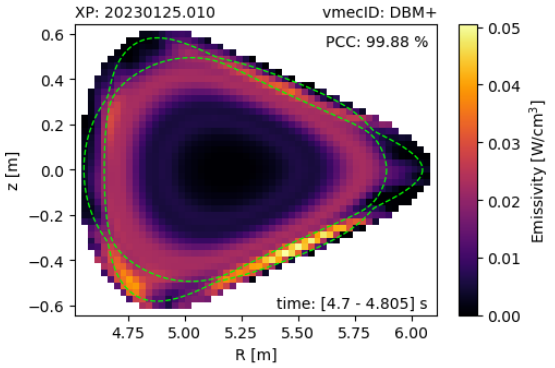

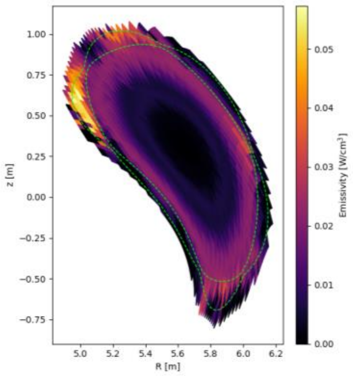

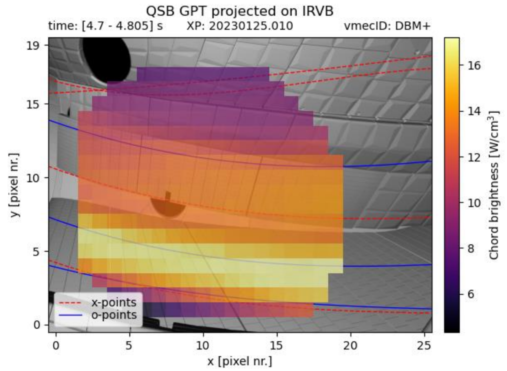

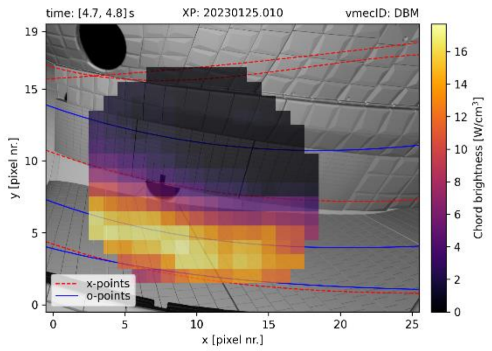

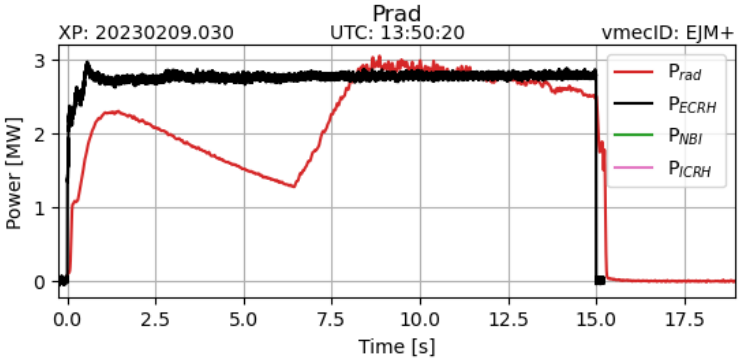

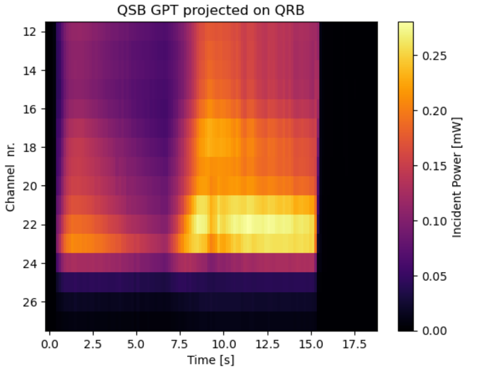

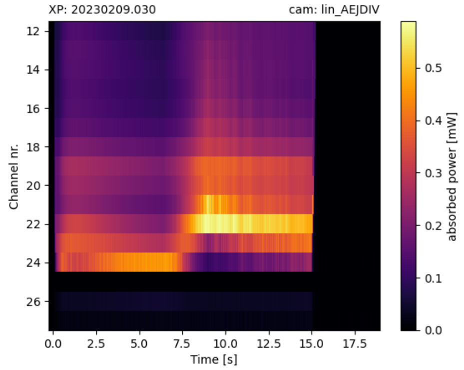

k_{bolo} factor

The line-integrated power on a given pixel scales with the pixel etendue E (roughly pinhole-to-foil projectied area) and the length (or volume) of the LoS crossing the plasma volume, d_{LoS}.

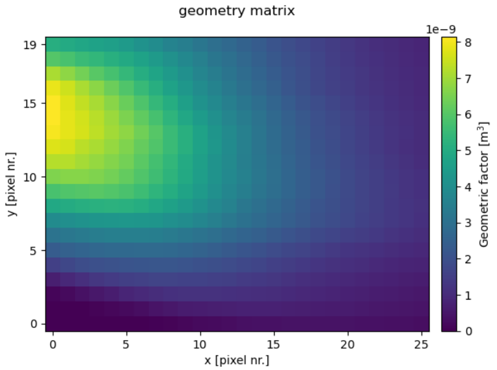

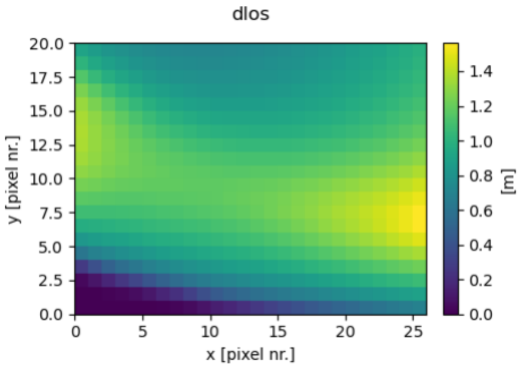

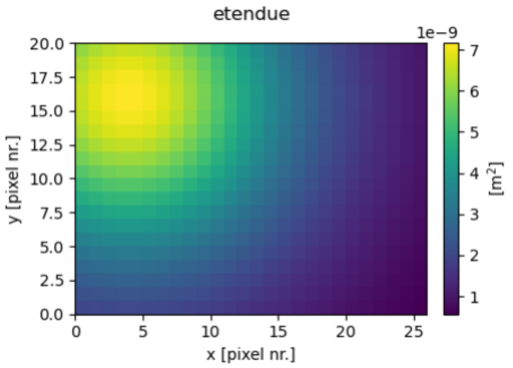

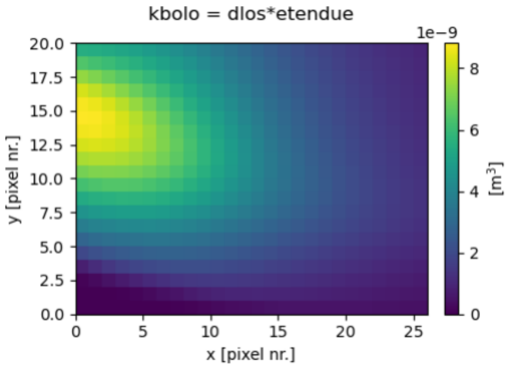

The raw power load data is usually divided by the so-called k_{bolo} factor, defined as the product of the two, to disentangle the plasma emissivity features from the specific camera geometry. This normalized quantity is named **chord brightness** P_{chord}.

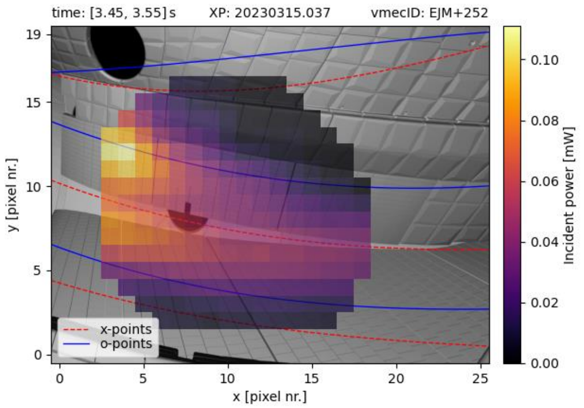

$$P_{chord} = \frac{P_{lin}}{d_{LoS} E}$$

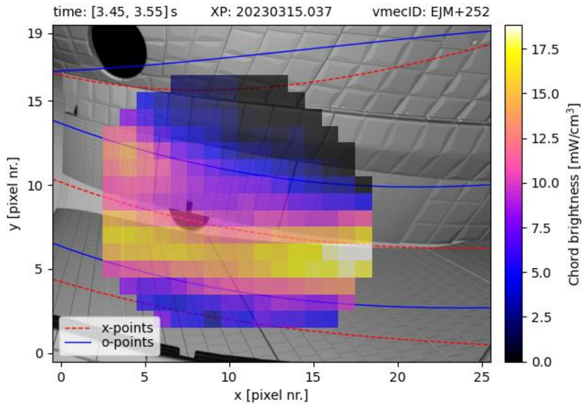

ICRH effect on P_{rad}

- ICRH power is radiatively dissipated
- W_{dia} is unaffected
- P_{rad} effect is localized in lower right island
- Magnetically connected to injection point
- Pattern without antenna is slightly different

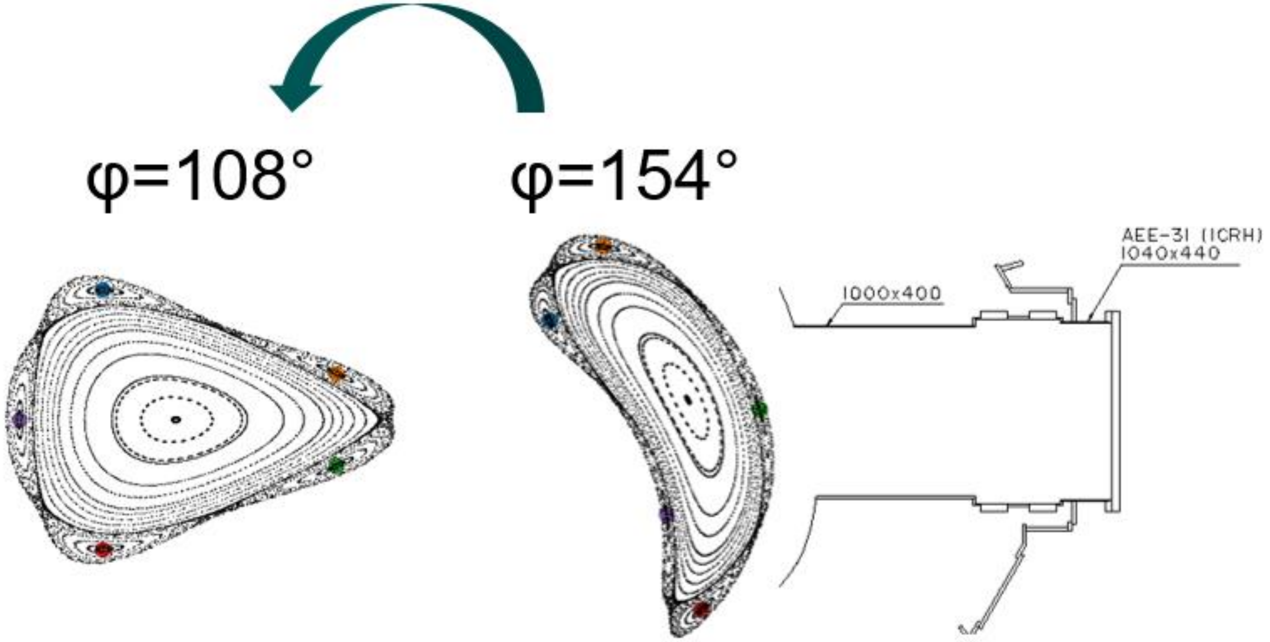

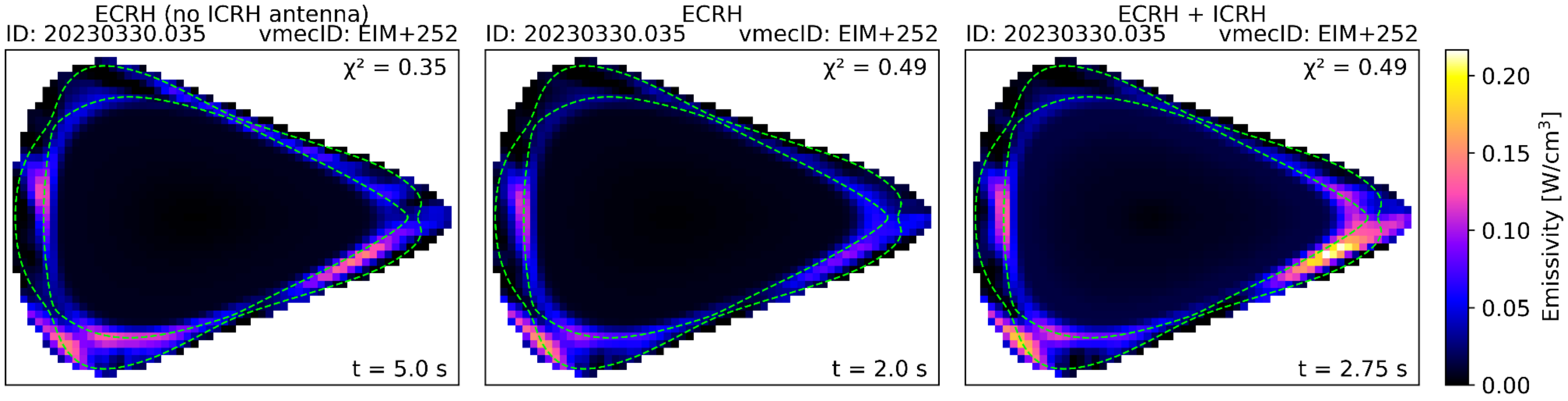

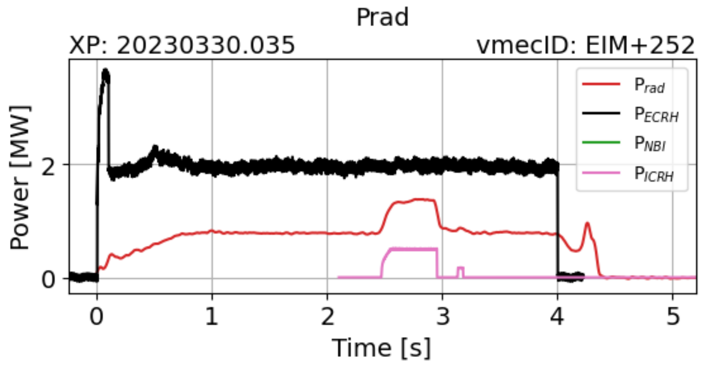

IRVB components

camera box (closed)

camera box (open)

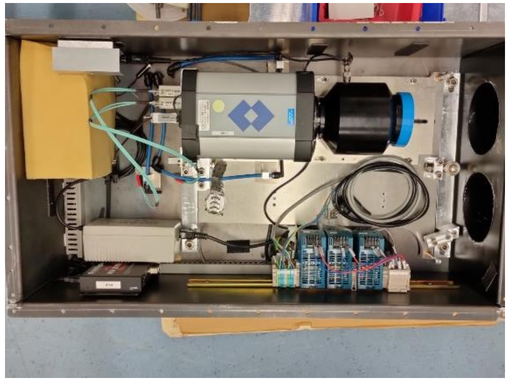

parabolic mirrors

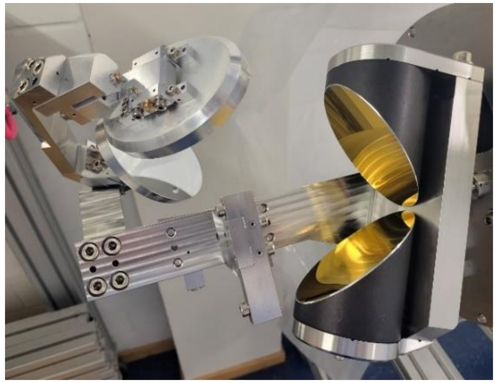

foil + frame

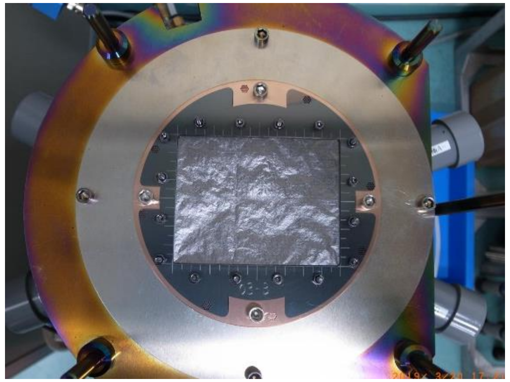

endoscope cap

foil (assembled)

endoscope front

torus hall